7

Theoretical Analyses of Photoinduced Electron Transfer from Aromatic Amino Acids to the Excited Flavins in Some Flavoproteins

Kiattisak Lugsanangarm[1], Nadtanet Nunthaboot[2], Somsak Pianwanit[1,3,*], Sirirat Kokpol[1,3] and Fumio Tanaka[1,4,*]

[1]*Department of Chemistry, Faculty of Science, Chulalongkorn University,*

[2]*Department of Chemistry, Faculty of Science, Mahasarakham University, Mahasarakham,*

[3]*Center of Excellence for Petroleum, Petrochemicals, and Advanced Materials, Chulalongkorn University, Bangkok,*

[4]*Laser Biochemistry Division, Institute for Laser Technology, Osaka,*

[1,2,3]*Thailand*

[4]*Japan*

1. Introduction

Electron transfer phenomena have been an important subjects in the fields of physics (Jortner & Bixon, 1999), chemistry (Mataga et al., 2005a, 2005b; Vogler et al., 2011) and biology (Marcus & Sutin, 1985; Gray & Winkler, 1996; Bendal, 1996). Photoinduced electron transfer (PET) plays an essential role in photosynthetic systems (Blankenship, 2002). In the last decade a number of new flavin photoreceptors have been found. Among six families of the photoreceptors, phototropins (Crosson & Moffat, 2001), cryptochromes (Giovani et al., 2003) and BLUF (blue-light sensing using flavin) contain flavins as the reaction center (Masuda & Bauer, 2002). The PET from Tyr to the excited isoalloxazine (Iso*) is considered as an initial step of the photo-regulation for photosynthesis in AppA (Masuda & Bauer, 2002; Laan et al., 2003) and pili-dependent cell motility in TePixD (Kita et al., 2005) and in Slr1694 (Masuda et al., 2004) photoactive bacteria.

Flavoproteins contain flavin mononucleotide (FMN), flavin adenine dinucleotide, and riboflavin as a cofactor and are ubiquitously distributed in various microorganisms, in leafy vegetables and specific tissues of other multicellular plants, and in the milk, brain, kidney, liver and heart of mammals, where they play an essential role in many redox reactions (Frago et al., 2008).

The fluorescence of flavins was first reported by Weber (1950), along with the fluorescence quenching of flavins by various substances, including aromatic amino acids. Since then many researchers have studied the photochemistry of flavins and flavoproteins (Silva &

* Corresponding Authors

Edward, 2006). The quenching of flavin fluorescence by an indole ring was reported with isoalloxazine-$(CH_2)_n$-indole dyads by McCormick (1977). Time-resolved fluorescence spectroscopy of flavins and flavoproteins has been reviewed by Berg and Visser (2001). However, a number of flavoproteins are practically non-fluorescent, but rather they emit fluorescence with very short lifetimes (sub-picoseconds) upon excitation with an ultra-short laser pulse (Mataga et al., 1998, 2000, 2002; Tanaka et al. 2007; Chosrowjan et al., 2007, 2008, 2010). In these flavoproteins tryptophan (Trp) and/or tyrosine (Tyr) residues always exist near the isoalloxazine ring (Iso). The remarkably fast fluorescence quenching in these flavoproteins was demonstrated to be caused by PET from Trp and/or Tyr to the excited state Iso (Iso*), by means of picosecond (Karen et al., 1983, 1987) and femtosecond (Zhong & Zewail, 2001) transient absorption spectroscopy. The PET phenomena in these flavoproteins are similar to the flavin photo-receptors (Crosson & Moffat, 2001; Masuda & Bauer, 2002), but had been discovered before the flavin photoreceptors.

Since the seminal works on electron transfer theory by Marcus (1956a, 1956b, 1964), several researchers have further developed the electron transfer theory (Hush, 1961; Sumi & Marcus, 1986; Bixon & Jortner, 1991, 1993; Bixon et al., 1994; Kakitani & Mataga, 1985; Kakitani et al., 1991, 1992). However, they have been modeled for PET in bulk solution and it is not clear whether these theories can be applicable to PET in proteins. Therefore, it is required to establish a method to quantitatively analyze PET in proteins.

In any electron transfer theories there are several parameters that are difficult to determine experimentally. The PET rates in flavoproteins have been analyzed experimentally with ultrafast fluorescence dynamics and theoretically by an electron transfer theory using the atomic coordinates obtained by molecular dynamics (MD) simulation. The procedure to determine the unknown PET parameters is as follows (Nunthaboot et al., 2008a, 2009a): (1) the time-dependent atomic coordinates of flavoproteins are obtained by MD simulation, (2) the PET rates are then calculated using a PET theory and the atomic coordinates with a set of trial PET parameters, (3) the parameters are then varied until the best-fit between the calculated and observed fluorescence decays is obtained, according to a non-linear least squares method.

In this review article we describe the results of quantitative analyses of PET in wild type (WT) flavodoxin and FMN binding proteins from *Desulfovibrio vulgaris*, Miyazaki F, and three relevant flavodoxin amino acid substitution mutants (isoforms) and two relevant FMN binding protein amino acid substitution mutants, respectively, and discuss the characteristics of the PET mechanism in flavoproteins.

Note that for brevity, unless stated otherwise, reference to flavodoxin and FMN binding proteins in this article refers to those from *Desulfovibrio vulgaris*, Miyazaki F.

2. Method of analysis of Photoinduced Electron Transfer (PET) in flavoproteins

2.1 Electron transfer theory in flavoproteins

All of the original PET theories were modeled for a system in solution. Here, we describe the PET theories that have been used for the flavoproteins. Electrostatic (ES) energy was first introduced by Nunthaboot et al. (2009a).

2.1.1 Marcus-Hush theory

When the j^{th} flavoprotein contains several PET donors, the PET rate from the k^{th} Trp and/or Tyr near Iso to Iso* by Marcus theory as modified by Hush (1961) (MH theory) is expressed by Eq. (1), and the energy diagram for MH theory is shown in Figure 1.

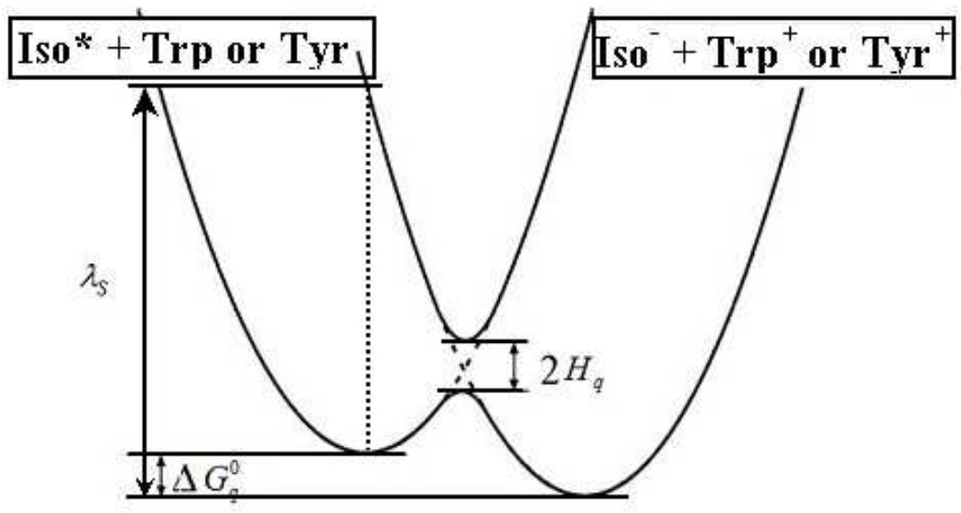

Fig. 1. Energy diagram for Marcus-Hush PET theory

$$k_{MH}^{jk} = \frac{2\pi}{\hbar}\frac{H_q^2}{\sqrt{4\pi\lambda_S^{jk}}}\exp\left[-\frac{\left\{\Delta G_q^0 - e^2/\varepsilon_{DA}R_{jk} + \lambda_S^{jk} + ES_j(k)\right\}^2}{4\lambda_S^{jk}k_BT}\right] \quad (1)$$

In Eq. (1), H_q is the electronic interaction energy between Iso* and Trp (q = Trp) or Tyr (q = Tyr). R_{jk} is the center to center (Rc) distance between Iso and the ET donor k in the j^{th} flavoprotein. $\hbar$, k_B, T and e are the reduced Planck constant, Boltzmann constant, temperature and electron charge, respectively. ε_{DA} is the static dielectric constant of medium between the PET donors and acceptor. $ES_j(k)$ is the net ES energy between the k^{th} aromatic ionic species and all other ionic groups in the j^{th} flavoprotein, as described below. λ_S^{jk} is the solvent reorganization energy of the Iso* and the k^{th} donor in the j^{th} flavoprotein, as shown by Eq. (2);

$$\lambda_S^{jk} = e^2\left(\frac{1}{2a_{Iso}} + \frac{1}{2a_q} - \frac{1}{R_{jk}}\right)\left(\frac{1}{\varepsilon_\infty} - \frac{1}{\varepsilon_{DA}}\right) \quad (2)$$

Here, a_{Iso} and a_q are the radii of Iso and the donor q (Trp or Tyr), assuming these reactants are spherical, and ε_∞ is the optical dielectric constant (a value of 2 being used). ε_{DA} is the static dielectric constant between Iso and a donor. The radii of Iso, Trp and Tyr were determined according to the following procedure. (1) The three dimensional sizes of lumiflavin for Iso, 3-methylindole for Trp, and p-methylphenol for Tyr were obtained by a semi-empirical molecular orbital method (PM3). (2) The volumes of these molecules were

determined as asymmetric rotors. (3) The radii of the spheres having the same volumes of the asymmetric rotors are obtained. The obtained radii by this procedure are a_{Iso} = 0.224 nm, a_{Trp} = 0.196 nm and a_{Tyr} = 0.173 nm.

The standard free energy gap (ΔG_q^0) was expressed with the ionization potential (E_{IP}^q) of the PET donor q (Trp or Tyr), as shown in Eq. (3).

$$\Delta G_q^0 = E_{IP}^q - G_{Iso}^0 \tag{3}$$

where G_{Iso}^0 is the standard Gibbs energy related to the electron affinity of Iso*. The values of E_{IP}^q for Trp and Tyr were 7.2 eV and 8.0 eV, respectively (Vorsa et al., 1999).

2.1.2 Kakitani-Mataga (KM) theory

The PET rate by Kakitani & Mataga (KM theory) is expressed as Eq. (4), which describes the PET rate for both adiabatic and non-adiabatic processes, whilst the MH and Bixon-Jortner (BJ) theories (see below) describe only adiabatic processes.

$$k_{KM}^{jk} = \frac{\nu_0^q}{1+\exp\left\{\beta^q(R_{jk}-R_0^q)\right\}}\sqrt{\frac{k_BT}{4\pi\lambda_S^{jk}}}\exp\left[-\frac{\left\{\Delta G_q^0 - e^2/\varepsilon_{DA}R_{jk} + \lambda_S^{jk} + ES_j(k)\right\}^2}{4\lambda_S^{jk}k_BT}\right] \tag{4}$$

Here ν_0^q is an adiabatic frequency, β^q is the PET process coefficient, and R_0^q is a critical distance between the adiabatic and non-adiabatic PET processes. These quantities depend only on q (Trp or Tyr). When $R_{jk} < R_0^q$ the ET process is adiabatic, whereas when $R_{jk} > R_0^q$ it is non-adiabatic. The other quantities are the same as those in the MH theory (section 2.1.1).

2.1.3 Bixon-Jortner (BJ) theory

The BJ theory describes the PET rates from various vibronic states, as shown in Eq. (5), while the MH and KM theories only describe the PET from the lowest vibrational state.

$$k_{BJ}^{jk} = \frac{2\pi}{\hbar}H_q^2\frac{\exp\left\{-\beta(R_{jk}-\sigma_q)-S\right\}}{\sqrt{2\pi\lambda_S^{jk}}}\sum_{i=0}^{n}\frac{S^i}{i!}\exp\left[-\frac{\left\{\Delta G_q^0 - e^2/\varepsilon_{DA}R_{jk} + \lambda_S^{jk} + i\hbar\langle\omega\rangle + ES_j(k)\right\}^2}{4\lambda_S^{jk}k_BT}\right] \tag{5}$$

$S = \lambda_V / \hbar\langle\omega\rangle$ is the vibronic coupling constant, where λ_V is the reorganization energy associated with the average frequency $\hbar\langle\omega\rangle$, n is the number of vibrational modes in the donor and σ_q is the van der Waals contact and is given by Eq. (6).

$$\sigma_q = a_{Iso} + a_q \tag{6}$$

The meanings of all the other notations are the same as that given in the MH theory (section 2.1.1).

2.2 Electrostatic (ES) energy between the photoproducts and ionic groups in a protein

Proteins, including flavoproteins, contain many ionic groups, which may influence the PET rate. The cofactor in the relevant flavoproteins is FMN, which has two negative charges at the phosphate. The ES energy between the Iso anion or donor k^{th} cation, and all the other ionic groups in the j^{th} flavoprotein is expressed by Eq. (7):

$$E_j(k) = \sum_{i=1}^{n_E} \frac{C_k \cdot C_{Glu}}{\varepsilon_0^j R_k(Glu-i)} + \sum_{i=1}^{n_B} \frac{C_k \cdot C_{Asp}}{\varepsilon_0^j R_k(Asp-i)}$$
$$+ \sum_{i=1}^{n_K} \frac{C_k \cdot C_{Lys}}{\varepsilon_0^j R_k(Lys-i)} + \sum_{i=1}^{n_R} \frac{C_k \cdot C_{Arg}}{\varepsilon_0^j R_k(Arg-i)} + \sum_{i=1}^{2} \frac{C_k \cdot C_P}{\varepsilon_0^j R_k(P-i)} \quad (7)$$

where n_E , n_B , n_K and n_R are the numbers of Glu, Asp, Lys and Arg residues, respectively, in the flavoprotein. Here, k = 0 for the Iso anion, and k > 0 for the donor cations. ε_0^j is the static dielectric constant inside the entire j^{th} flavoprotein, which should be different from ε_{DA} . C_k is the charge of the aromatic ionic species k, and is -e for k = 0 (Iso anion), +e for k > 1. C_{Glu} (= - e), C_{Asp} (= - e), C_{Lys} (= + e), C_{Arg} (= + e) and C_P (= - e) are the charges of Glu, Asp, Lys, Arg and phosphate anions, respectively. It was assumed that these groups are all in an ionic state in solution. The pK_a values of the ionic amino acids in water are 4.3 in Glu, 3.9 in Asp, 10.5 in Lys and 12.5 in Arg. However, as residues within proteins these pK_a values may be modified in the range of ± 0.3. His displays a pK_a of 6.0 in water. All fluorescence measurements were performed in 0.1 M phosphate buffer at pH 7.0, where His should be neutral. Distances between the aromatic ionic species k and the i^{th} Glu are denoted as $R_k(Glu-i)$, those between k and the i^{th} Asp are denoted as $R_k(Asp-i)$, and so on. $ES_j(k)$ is expressed in Eq. (8);

$$ES_j(k) = E_j(0) + E_j(k) \quad (8)$$

2.3 Observed ultrafast fluorescence dynamics of flavodoxins and FMN binding proteins

Ultrafast fluorescence dynamics of flavodoxins and FMN binding proteins have been measured by means of a fluorescence up-conversion method (Mataga et al., 2002; Chosrowjan et al., 2007, 2008, 2010). The fluorescence decay functions of the WT flavodoxin, the two single substitution isoforms, Y97F and W59F, and the double substitution, Y97F/W59F (DM), are represented by Eq. (9), whilst the fluorescence decays of the WT FMN binding protein and the four single substitution isoforms, E13T, E13Q, W32Y and W32A, are represented by Eq. (10).

$$F_{FD}^j(t) = \sum_{i=1}^{n} \alpha_{FDi}^j \exp(-t/\tau_{FDi}^j) \quad (j=1, \text{WT}; j=2, \text{Y97F}; j=3, \text{W59F}; j=4, \text{Y97F/W59F}) \quad (9)$$

$$F_{FBP}^j(t) = \sum_{i=1}^{n} \alpha_{FBPi}^j \exp(-t/\tau_{FBPi}^j) \; (j=1, \text{WT}; j=2, \text{E13T}; j=3, \text{E13Q}; j=4, \text{W32Y}; j=5, \text{W32A}) \quad (10)$$

In Eq. (9), n = 1 or 2, and in Eq. (10) n = 1 to 3, depending on the protein system, j. The decay parameters are listed in Table 1. The experimental decay of the WT flavodoxin contains an additional lifetime component with 500 ps. However, it was interpreted to be free FMN dissociated from the protein. The average lifetime values, τ_{AV}^{k}, were obtained from $\tau_{AV}^{j} = \sum_{i=1}^{n} \alpha_i^j \tau_i^j$ and are listed in the last line of Table 1. The decays with n greater than 1 display non-exponential function.

Decay parameter	Flavodoxin[b]				FMN binding protein[c]				
	WT	Y97F	W59F	DM[d]	WT	E13T	E13Q	W32Y	W32A
τ_1^j (ps)	0.157	0.254	0.322	18	0.167	0.107	0.134	3.4	30.1
(α_1^j)	(1.0)	(0.85)	(0.83)	(1.0)	(0.96)	(0.86)	(0.85)	(0.23)	(1.0)
τ_2^j (ps)	-	4.0	5.5	-	1.5	1.5	0.746	18.2	-
(α_2^j)	-	(0.15)	(0.17)	-	(0.04)	(0.12)	(0.12)	(0.74)	-
τ_3^j (ps)	-	-	-	-	-	30	30	96	-
(α_3^j)	-	-	-	-	-	(0.02)	(0.03)	(0.03)	-
τ_{AV}^{k} [e] (ps)	0.157	0.816	1.20	18	0.22	0.872	1.10	17.1	30.1

[a]The observed flavodoxin and FMN binding protein decay functions are expressed in Eqs. (9) and (10), respectively.
[b]Data were taken from the work by Mataga et al. (2002).
[c]Data were taken from the works by Chosrowjan et al. (2007, 2008, 2010).
[d]DM denotes the Y97F/W59F double mutant.
[e]Averaged lifetimes were obtained by $\tau_{AV}^{j} = \sum_{i=1}^{n} \alpha_i^j \tau_i^j$.

Table 1. Fluorescence decay parameters of the flavodoxin and FMN binding protein isoforms from *Desulfovibrio vulgaris*, Miyazaki F [a]

2.4 Determination of the PET parameters

The calculated decay function in the j^{th} protein system is expressed by Eq. (11).

$$F_{calc}^{j}(t) = \left\langle \exp\left\{ -\sum_{k=1}^{m} k_{ET}^{jk}(t')t \right\} \right\rangle_{AV} \tag{11}$$

$\langle ... \rangle_{AV}$ means the averaging procedure of the exponential function in Eq. (11) over t'. In Eq. (11) we assumed that the decay function at every instant of time, t', during the MD simulation time range can always be expressed by an exponential function, and thus the MD

simulation time range must be much longer than experimental decay time range. In Eq. (11) m is the total number of PET donors in the j^{th} flavoprotein. In MH theory, the unknown PET parameters were H_q (q = Trp and Tyr), G^0_{Iso}, ε_{DA} and ε^j_0, whilst in KM theory they are ν^q_0, β^q, and R^q_0 for Trp and Tyr, G^0_{Iso}, ε_{DA} and ε^j_0, and in BJ theory they are H_q (q = Trp or Tyr), β, λ_V, $\hbar\langle\omega\rangle$, G^0_{Iso}, ε_{DA} and ε^j_0. These parameters were determined so as to obtain the minimum value of χ^2, as defined by Eq. (12), by means of a non-linear least squares method, according to the Marquardt algorithm.

$$\chi^2 = \frac{1}{N_j N_F} \sum_{j=1}^{N_j} \sum_{i=1}^{N_F} \frac{\left\{ F^j_{calc}(t_i) - F^j_{obs}(t_i) \right\}^2}{F^j_{calc}(t_i)} \tag{12}$$

Here, N_F denotes the number of time intervals in the fluorescence decay, and N_j is the total number of flavoproteins for simultaneous analysis.

3. Flavodoxins from *Desulfovibrio vulgaris*, Miyazaki F

3.1 Homology modeling

Flavodoxins are small flavoproteins with a molecular weight of 15 - 23 kDa that have been isolated from a variety of microorganisms. Flavodoxins are considered to function as electron-transport proteins in various metabolic pathways (Sancho, 2006). They contain one molecule of non covalently-bound FMN (see Chart 1) as a cofactor, and exhibit a highly negative reduction potential for the semiquinone / hydroquinone couple of FMN, and accordingly the semiquinone state is stable. The redox properties of FMN in flavodoxins are considerably different from those of the free FMN.

The biochemical properties of flavodoxin from *Desulfovibrio vulgaris*, strain Miyazaki F were first characterized by Kitamura et al. (1998). The dissociation constant of FMN is 0.38 nM, which is ~1.6-fold higher than that in the related flavodoxin from Desulfovibrio vulgaris Hildenborough (0.24 nM). The redox potential of these two closely related flavodoxins is also slightly different, being E_1 = -434 and -440 mV for the Miyazaki and Hildenborough forms, respectively, for the oxidized-semiquinone reaction of flavodoxin, and E_2 = -151 and -143 mV for the semiquinone-2-electron reduced reaction, respectively (Kitamura et al., 1998). Recently, the three-dimensional structures of numerous flavodoxins have been determined, including Desulfovibrio vulgaris Hildenborough (Watenpauph, 1973) and the flavodoxins from Anacystis nidulans (Drennan et al., 1999), Clostridium beijerinckii (Ludwig et al., 1997), Escherichia coli (Hoover & Ludwig, 1997), Anabaena 7120 (Burkhart et al., 1995) a red algae (Fukuyama et al., 1992) Chondrus crispu (Fukuyama et al., 1990) and H. pylori (Freigang et al., 2002) by X-ray crystallography. The structure of flavodoxin, however, has not yet been determined, although the primary structure is known (Kitamura et al., 1998).

The ultrafast fluorescence dynamics of flavodoxins (Mataga et al., 2002) have been extensively investigated in the WT and the Y97F, W59F and W59F/Y97F (DM) substitution isoforms, as described above.

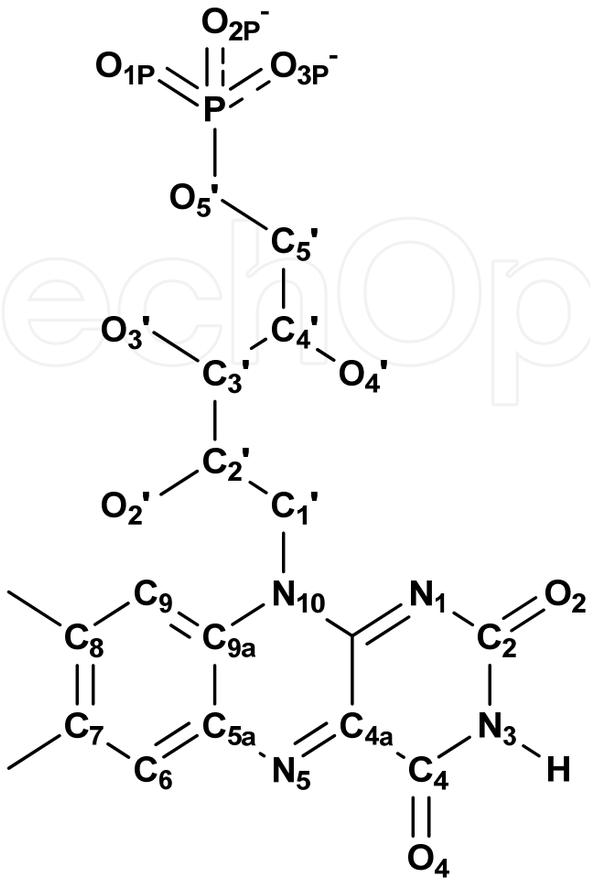

Chart 1. Chemical structure of FMN and its atom notations.

3.2 Three-dimensional structures of four flavodoxin isoforms

The protein structures of the WT, single amino acid substitution (Y97F and W59F) and the double amino acid substitution (W59F/Y97F; DM) isoforms have been determined by homology modeling method with the Modeler Module of the Discovery Studio 2.0 software package (http://www.discoverystudios.com) using the flavodoxin *Desulfovibrio vulgaris*, strain Hildenborough structure (PDB code: 1J8Q) as the template. This protein displays 66% amino acid sequence identity and 79% similarity to the WT flavodoxin of Miyazaki reviewed herein. The validities of the structures were examined with a Verified3D analysis (visit for the method, www.proteinstructures.com by Prof. Salam Al-Karadaghi). Verify3D assigns each residue a structural class based on its location and environment (alpha, beta, loop, polar, apolar etc). Then, a database generated from good structures is used to obtain a score for each of the 20 amino acids in this structural class. Figure 2 shows the Verified3D scores at each amino acid residue, where the quality of the structures is satisfactory.

MD simulations were performed for 10 ns in order to investigate the dynamic properties of the proteins and the important interactions that are involved in the binding of the FMN cofactor to the proteins. Figure 3 shows the three-dimensional structures in water that were obtained by MD simulation.

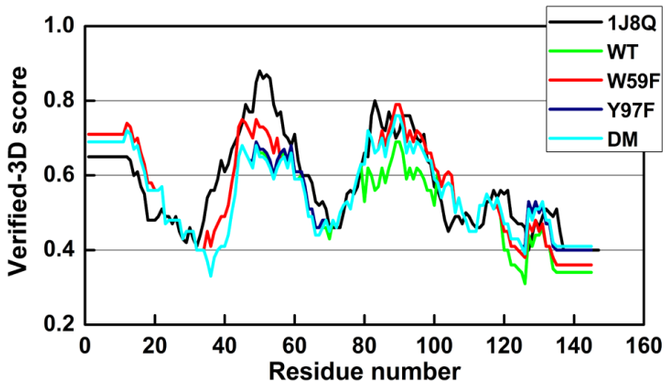

Fig. 2. Verifyed-3D analysis of the template (1J8Q), and the four isoforms of *Desulfobivrio vulgaris*, strain Miyazaki F., that were constructed by the homology modeling. The compatibilities of amino acids in their environments are indicated by the positive scores. Data taken from Lugsanangarm et al. (2011a).

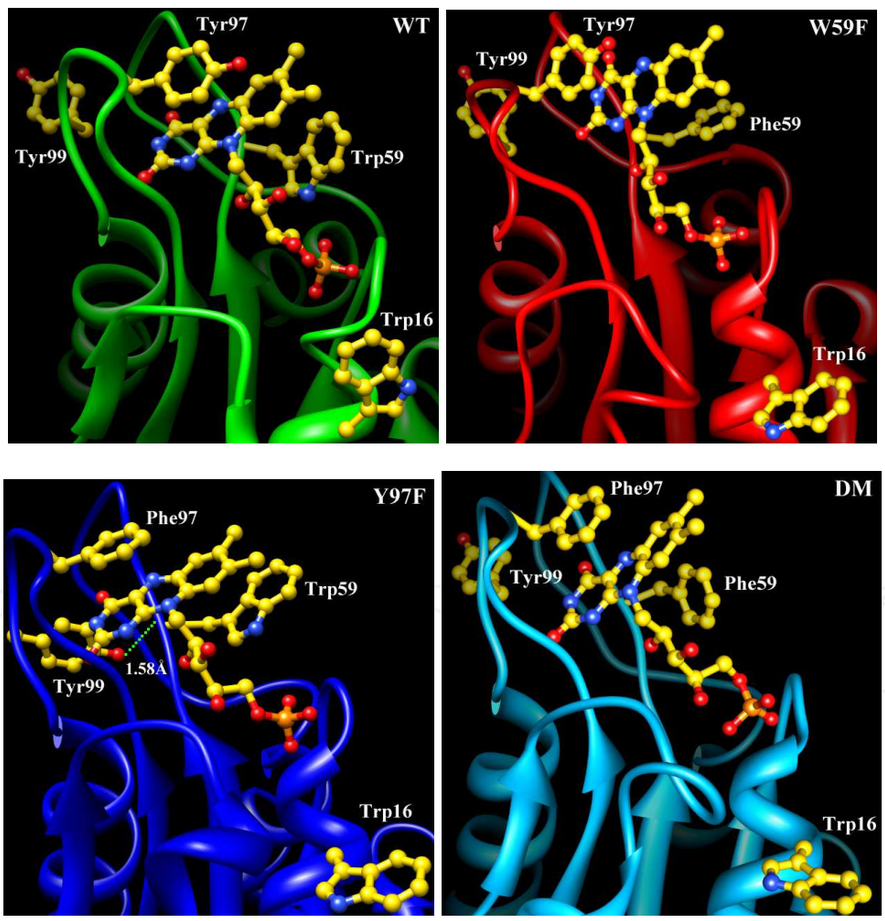

Fig. 3. Structures of four flavodoxin isomers. In the WT isoform, Trp59, Tyr97, Tyr99 and Trp16 are potential PET donors to Iso*, whilst these are Trp59, Tyr99 and Trp16 in the Y97F isomer and Tyr97, Tyr99 and Trp16 in the W59F isomer. In the DM, Tyr99 and Trp16 are the potential PET donors. Data were taken from Lugsanangarm et al. (2011a).

3.3 Decomposition free energy analysis of amino acid residues at the FMN binding site

In order to evaluate the important amino acid residues for FMN binding, the decomposition free energy per amino acid residue has been obtained. Figure 4 shows the decomposition energy of FMN from FMN-apoflavodoxin complexes. The amino acids near FMN are categorized into three groups, the 10-loop, 60-loop and 90-loop regions (see Figure 4). The decomposition energy is highest in the amino acids in the 10-loop regions (Ser9, Thr10, Thr11, Gly12 and Asn13 and Thr14) in all isoforms (Figure 4). All amino acids in the 10-loop region form hydrogen bonds with the FMN side chain viz: Ser9OH with O_{3P}, Thr10NH(peptide) with O_{1P}, Thr11OH with O_{2P}, Thr11NH(peptide) with O_{2P} and O_{1P}, Gly12NH(peptide) with O_{2P}, Asn13NH(peptide) with O_{2P}, Thr14OH with O_{3P} and Thr14NH(peptide) with O_{3P} (see Chart 1 for atom notations). These hydrogen bond interactions are considered to contribute the largest proportion of the decomposition free energy. Among the four flavodoxin isoforms, the decomposition energy is highest in Y97F (-9.30 kcal/mol), followed by W59F (-9.25 kcal/mol), DM (-8.60 kcal/mol) and is lowest in the WT (-8.54 kcal/mol).

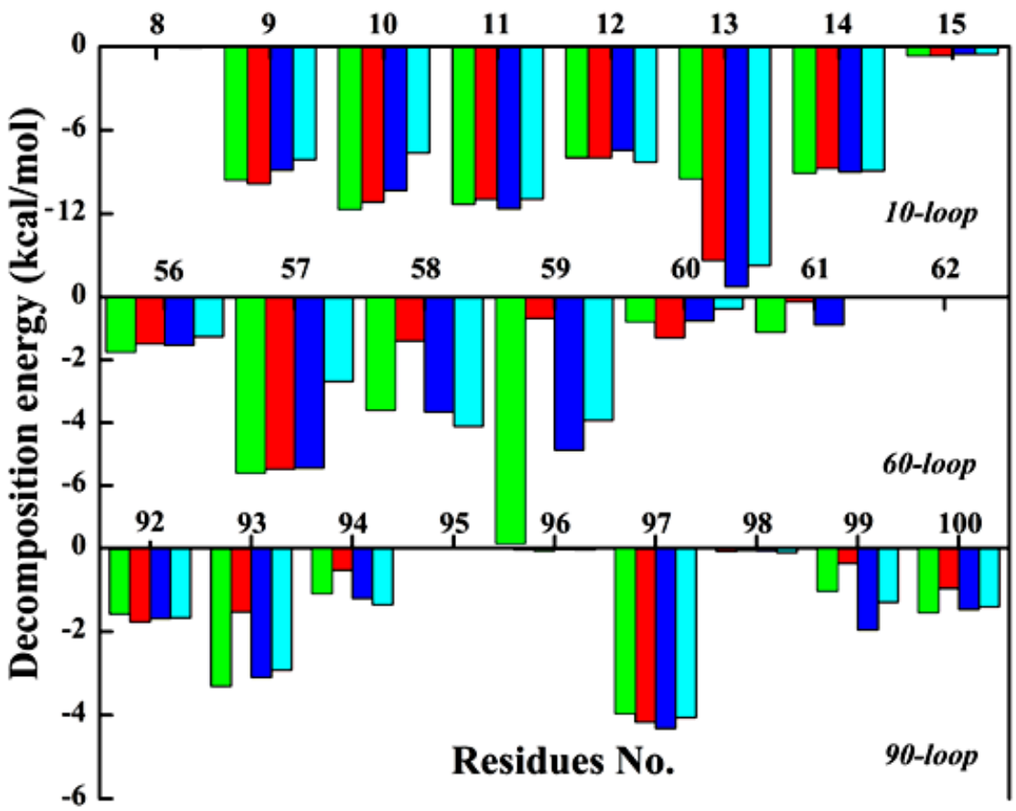

Fig. 4. Decomposition free energy of amino acid residues at the FMN binding site of the four flavodoxin isoforms. The energies are shown with green bars for WT, red bars for W59F, deep blue bars for Y97F and light blue bars for DM. Data were taken from Lugsanangarm et al. (2011a).

3.4 Structural dynamics of flavodoxins

Potential PET donors in the WT flavodoxin are Trp59, Tyr97 and Tyr99 and Trp16. The protein dynamics of these flavodoxin isoforms have been examined by viewing the time-dependent changes in the Rc distances and the inter-planar angles between Iso and these donors. Figure 5 shows the time-evolutions of Rc in the four different flavodoxin isoforms, where the Rc distances clearly fluctuate rapidly but are mostly within ± 10% of the mean values. In the DM the Rc values of Tyr99 and Trp16 vary with long periods in addition to the rapid fluctuation. Since the bulky Tyr97 and Trp59 residues are both replaced by the smaller Phe residue in the DM then the space around Iso may be increased compared to that in the WT, and so may account for the marked fluctuation in the Rc distances of Tyr99 and Trp16. Figure 6 shows the time-evolutions of the inter-planar angles in the WT flavodoxin, where the variation of the inter-planar angles is about ± 30 deg around the mean. The derived mean Rc and edge-to-edge (Re) distances and inter-planar angles over the MD time range are listed in Table 2. The Rc distance was shortest in Tyr97 and then Trp59 in all four flavodoxin isoforms, whilst Tyr99 and Trp16 are quite far from Iso. The inter-planar angle of Trp 59 in the WT is -43 deg, while it is 73 deg in Y97F.

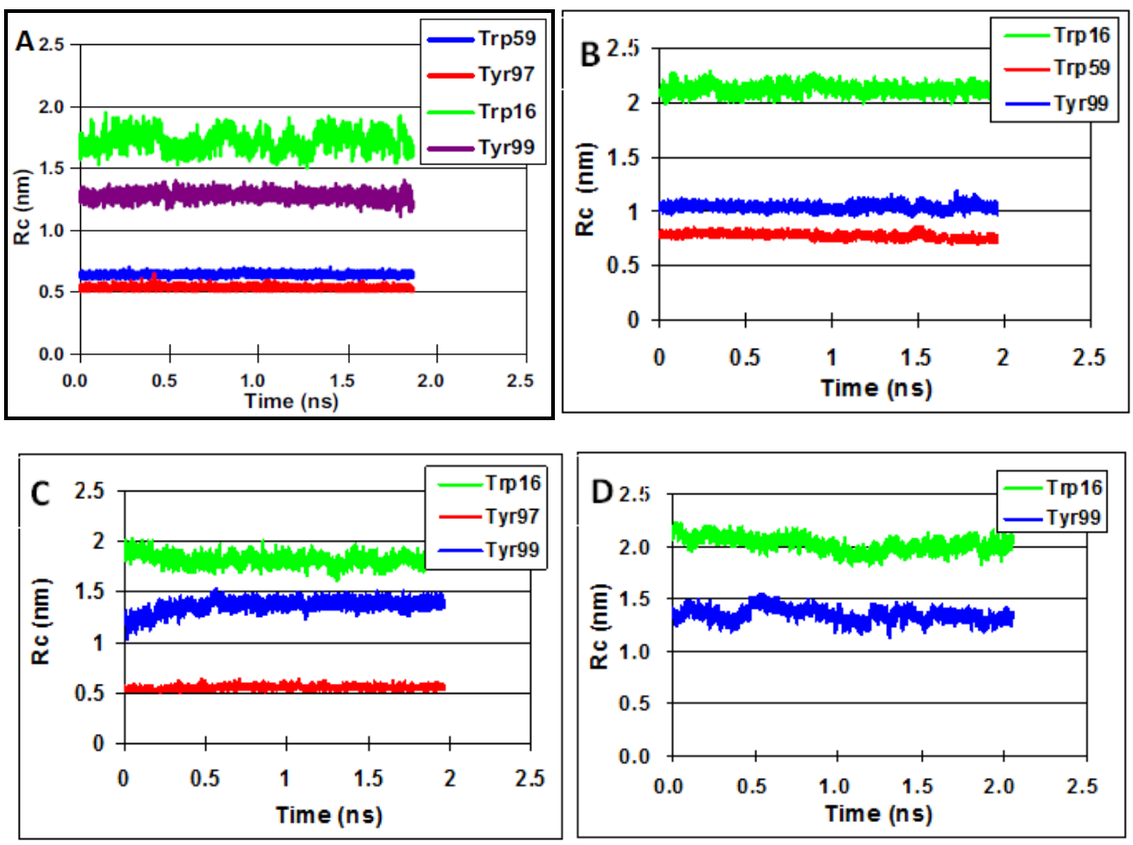

Fig. 5. Time evolution of the Rc distance between Iso and the indicated potential PET donor in the (A) WT, (B) Y97F, (C) W59F and (D) DM (Y97F/W59F) flavodoxin isoforms. Figure 5A was taken from Lugsanangarm et al. 2011b. Figures 5B, 5C and 5D were taken from Lugsanangarm et al. 2011c.

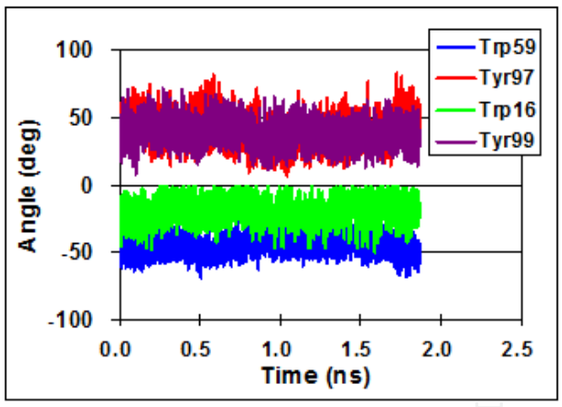

Fig. 6. Time evolution of the inter-planar angle between Iso and the four potential PET donors in the WT flavodoxin. Data were taken from Lugsanangarm et al. (2011b).

Protein	Donor	*Rc*[b] (nm)	*Re*[c] (nm)	Angle[d] (deg)
WT[e]	Trp59	0.642	0.247	-42.8
	Tyr97	0.536	0.301	14
	Tyr99	1.28	0.533	23.5
	Trp16	1.72	1.18	-18.1
Y97F[f]	Trp59	0.858	0.264	73.1
	Tyr99	1.12	0.329	55.7
	Trp16	2.1	1.51	53
W59F[g]	Tyr97	0.577	0.259	14
	Tyr99	1.34	0.513	28.9
	Trp16	1.85	1.42	-24.5
DM[h]	Tyr99	1.35	0.496	-28.6
	Trp16	2.02	1.44	30.9

[a] The means values are listed, which were obtained by taking the average over the MD simulation time (2 ns with 0.1 ps time intervals). Data are taken from Lugsanangarm et al. (2011c).
[b] Center to center and [c] edge to edge distances between Iso and the aromatic amino acids.
[d] Inter-planar angles between Iso and the aromatic amino acids.
[e] The data are taken from Lugsanangarm et al. (2011b).
[f] Tyr97 is replaced by Phe.
[g] Trp59 is replaced by Phe.
[h] Both Tyr97 and Trp59 are replaced by Phe

Table 2. Geometrical factors in the four flavodoxin isoforms[a]. Data were taken from Lugsanangarm et al. (2011c).

3.5 The PET mechanism in flavodoxins

3.5.1 Analysis of PET with crystal structures of flavoproteins

The PET analysis in flavoproteins first starts with their crystal structures (Tanaka et al., 2007, 2008). The logarithms of the averaged PET rate (inverse of the averaged lifetimes) in ten flavoprotein systems are plotted against the Re and Rc distances. The logarithms of the PET

rates can be expressed with two straight lines when Rc instead of Re is used (see Figure 7). At longer distances the PET rate rapidly decreases with increasing Rc distances, while at shorter distances it decreases slowly with the same sized increments in the Rc value. When Re is used in place of Rc as the distance measure, no such clear distance-dependence is observed in the flavoprotein systems. According to Moser et al. (1992), the logarithm of the PET rate in photosynthesis systems linearly decreases with increasing Re. However, the time domain of the PET rates in their work is much longer than the one in the flavoprotein systems. It is conceivable then that the logarithm of the PET rate in photosynthesis systems increases more slowly with Rc when the distances become shorter.

The PET in the fast phase with low slope was interpreted to be "Coherent PET", where the PET takes place to the Franck-Condon state of Iso* from Trp or Tyr (Mataga et al., 2002).

Of the ten flavoproteins evaluated, the PET donors with a Rc distance of less than 1 nm were all Trp residues, except for Tyr97 in flavodoxin with an exceptionally low PET rate at an Rc value of 0.57 nm. The low rate in Tyr97 was elucidated by the higher ionization potential of Tyr compared to Trp (Tanaka et al., 2007, 2008). Moreover, the agreement between $\ln k_{ET}^{obs}$ and $\ln k_{ET}^{calc}$ were the highest with KM theory (Figure 7) compared to that MH theory (Sumi & Marcus, 1986) or BJ theories (not shown).

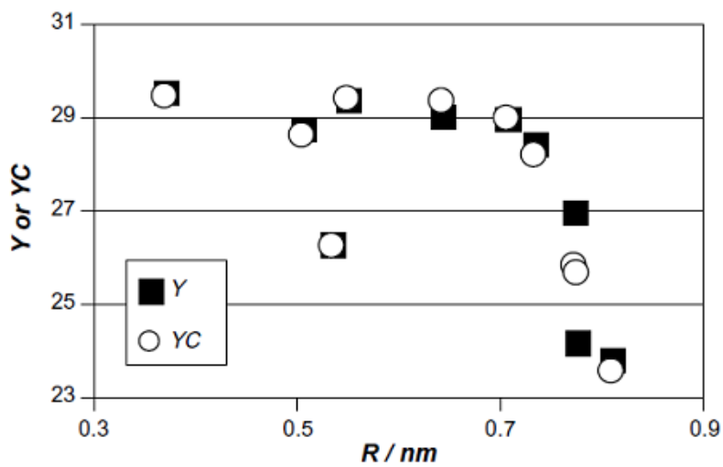

Fig. 7. $\ln k_{ET}$ vs. Rc plot for the observed and KM theory calculated PET rates of 10 flavoprotein systems. Y and YC represent $\ln k_{ET}^{obs}$ and $\ln k_{ET}^{calc}$, respectively, where k_{ET}^{obs} and k_{ET}^{calc} are the observed and KM theory calculated PET rates, respectively. Data are taken from Tanaka et al. (2008).

3.5.2 PET analysis with MD snapshots of four flavodoxin isoforms

The PET analysis from ultrafast fluorescence dynamics was first conducted by Nunthaboot et al. (2008a, 2009a). Time-dependent PET rates in FMN binding proteins were evaluated from the atomic coordinates of the protein as obtained by MD simulation. All PET theories contain several PET parameters that cannot be experimentally determined. Rather these parameters are numerically determined by a non-linear least-square method, as described in Section 2.4.

Fluorescence decay functions of four flavodoxin isoforms (WT, Y97F, W59F and DM) were simultaneously analyzed, with the atomic coordinates of these proteins obtained by MD simulation and KM theory, by Lugsanangarm et al. (2011b, 2011c). The PET parameters common among these flavodoxin systems are listed in Table 3. Ultrafast decay functions of the flavodoxins are expressed by Eq. (9) using the decay parameters listed in Table 1. It is noted that the values of ν_0 and β are quite different between Trp and Tyr, which is related to the electron coupling terms in the KM theory. The quantum basis for the difference is described by Nunthaboot et al. (2008b). In these works it is assumed that the static dielectric constant varies with the protein systems. Table 4 lists the static dielectric constants inside each protein. The dielectric constant of the WT flavodoxin is greatest among the four systems, and that of the DM is the lowest. This is reasonable because Iso in the WT flavodoxin is sandwiched between the polar Trp59 and Tyr97 residues, while both of them are replaced by the non-polar Phe in the DM. Thus, in the DM isoform Iso should be in a relatively non-polar environment, whilst in the Y97F and W59F isoforms the Iso residue may be in a moderately polar environment.

System	ν_0 (ps^{-1})		β (nm^{-1})		R_0 (nm)		G^0_{Iso} (eV)	ε_{DA}
	Trp	Tyr	Trp	Tyr	Trp	Tyr		
Flavodoxin[b]	3090	2460	55.6	9.64	0.772	0.676	7.60	-
FMN binding protein[c]	1016	197	21.0	6.25	0.663	0.499	6.71	2.19

[a]Physical meanings of the PET parameters are described at Section 3.1. The PET parameters in the Table are common among the four isoforms of flavodoxin (WT, W59F, Y97F and DM), and were obtained according to the procedure described at Section 3.4.
[b]For flavodoxins, the four isoforms (WT, Y97F, W59F, DM) were simultaneously analyzed. Data are taken from Lugsanangarm et al. (2011b, 2011c).
[c]For the FMN binding proteins, the five isoforms (WT, E13T, E13Q, W32Y and W32A) were simultaneously analyzed.

Table 3. The best-fit PET parameters[a] . Data are taken from Nunthaboot et al. (2008a, 2009a, 2011).

	Flavodoxin [b]				FMN binding protein [c]				
Variant	WT	Y97F	W59F	DM	WT	E13T	E13Q	W32Y	W32A
ε_0^j	5.85	4.78	4.04	2.28	14.8	5.99	6.69	5.89	6.29

[a] Dielectric constants, ε_0^j, are determined according to the procedure described at Section **3.4**

[b] The WT, Y97F, W59F and DM (Y97F/W59F) flavodoxin isoforms were simultaneously analyzed. Data are taken from Lugsanangarm, et al. (2011b, 2011c)
[c] The WT, E13T, E13Q, W32Y, W32A FMN binding protein isoforms were simultaneously analyzed.

Table 4. Dielectric constant inside the protein [a] Data taken from Lugsanangarm et al. (2011c) for Flavodoxin, and Nunthaboot et al. (2011).

3.5.3 Dynamics of the PET Rate and related physical quantities in flavodoxins

Time-dependent changes in the PET rates of the four flavodoxin isoforms are shown in Figure 8. n the WT and Y97F isoforms, the PET rates from Trp59 are the fastest even though

the Rc distance between Iso and Tyr97 in the WT is shorter (see Table 2). The mean PET rates over the MD time range (2 ns with 0.1 ps intervals) are listed in Table 5 along with the other mean physical quantities. The mean PET rate is fastest from Trp59 in WT and then in Y97F, as mentioned above, and is then followed by Tyr97 in the W59F isoform. The PET rates from Trp16 and Tyr99 are always negligibly slow.

The net ES energy, $ES_j(k)$, markedly varied from -0.00159 eV in Trp59 (Y97F) to 3.42 eV in Tyr99 (W59F), while λ_S^{jk} varied from 0.377 eV in Trp16 (DM) to 2.06 eV in Tyr99 (WT), and the ES energy between the donor and acceptor, $-e^2 / \varepsilon_0^j R_{jk}$, varied from -0.652 eV in Tyr97 (W59F) to -0.142 eV in Trp16 (Y97F). The amount of the variation is largest in the net ES energies. The dielectric constant between the Iso anion and the donor cation, ε_{DA}, is not introduced in the PET analysis for flavodoxins.

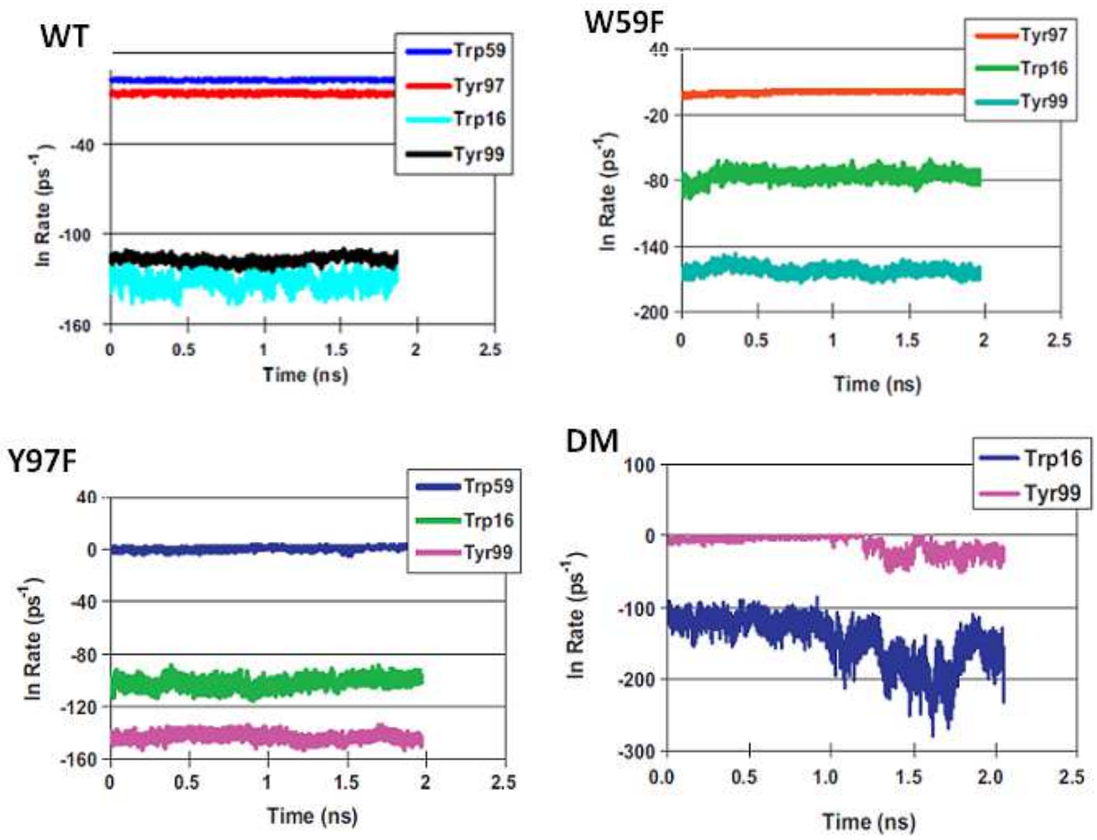

Fig. 8. The PET rates from Trp and/or Tyr to Iso* in four flavodoxin isoforms. Figure for WT was taken from Lugsanangarm (2011b). Figures for W59F, Y97F and DM were taken from Lugsanangarm (2011c).

Physical quantity	WT				W59F		
	Trp59	Tyr97	Trp16	Tyr99	Tyr97	Trp16	Tyr99
k_{KM}^{jk} (ps^{-1})[b]	7.10	1.26 x 10^{-3}	-	-	3.13	-	-
$\ln k_{KM}^{jk}$	1.96	−6.68	−125	−115	1.14	−69.10	−156
λ_S^{jk} (eV)[c]	1.53	1.54	1.99	2.06	1.20	1.54	1.59
$ES_j(k)$ (eV)[d]	−0.0172	−0.0942	2.73	2.71	−0.219	0.984	3.42
ΔG_q^0 (eV)[e]	−0.467	0.333	−0.467	0.333	0.333	−0.467	0.333
$-e^2 / \varepsilon_0^j R_{jk}$ (eV)[f]	−0.384	−0.460	−0.144	−0.193	−0.652	−0.196	−0.263
$-\Delta G_T^0(jk)$ (eV)[g]	0.868	0.221	−2.12	−2.86	0.583	−0.321	−3.49

Table 5A. Mean physical quantities related to the PET in the WT and W59F[a] flavodoxin isoforms[a]. Data were taken from Lugsanangarm et al. (2011c).

Physical quantity	Y97F			DM	
	Trp59	Trp16	Tyr99	Trp16	Tyr99
k_{KM}^{jk} (ps^{-1})[b]	4.95	-	-	-	7.43 x 10^{-2}
$\ln k_{KM}^{jk}$	1.60	−96.5	−134	−95.0	−2.60
λ_S^{jk} (eV)[c]	1.47	1.81	1.74	0.377	0.385
$ES_j(k)$ (eV)[d]	−0.00159	1.20	3.26	2.13	0.0131
ΔG_q^0 (eV)[e]	−0.467	−0.467	0.333	−0.467	0.333
$-e^2 / \varepsilon_0^j R_{jk}$ (eV)[f]	−0.386	−0.142	−0.289	−0.313	−0.470
$-\Delta G_T^0(jk)$ (eV)[g]	0.855	−0.594	−3.31	−1.35	0.124

[a]Physical quantities were obtained with the PET parameters listed in Table 3. Mean values are from over the MD time range (2 ns with 0.1 ps intervals).
[b]KM evaluated PET rates are given by Eq. (4).
[c]Solvent reorganization energy, as given by Eq. (2).
[d]Net ES energy, as given by Eq. (8).
[e]Standard free energy gap, as given by Eq. (3).
[f]ES energy between the Iso anion and the donor cation.
[g]Total free energy gap, as given by Eq. (12).

Table 5B. Mean physical quantities related to the PET in the Y97F and DM flavodoxin isoforms[a]. Lugsanangarm et al. (2011c)

4. Protein dynamics of FMN binding proteins

The FMN binding protein from *Desulfovibrio vulgaris* (Miyazaki F) is considered to play an important role in the electron transport process in the bacterium, but the whole picture of the electron flow and coupling of the redox proteins is not yet clear (Kitamura et al., 1998). Three-dimensional structures of the FMN binding protein from *D. Vulgaris* (Miyazaki F) were determined by X-ray crystallography (Suto et al., 2000) and NMR spectroscopy (Liepinsh et al., 1997). According to these structures, Trp32 is the closest residue to Iso

followed by Tyr35 and then Trp106. To examine the effect of Trp32 on the PET rate in the FMN binding protein, Trp32 was replaced by Tyr (W32Y) or Ala (W32A), and further the single negative charge at residue 13, glutamate 13 (E13) was replaced by either Thr (E13T) or Gln (E13Q). The crystal structures of E13T and E13Q were determined by X-ray crystallography (Chosrowjan et al. 2010). The dynamic behavior of these FMN binding protein isoforms were studied by MD simulation (Nunthaboot et al., 2008a, 2009a, 2011), and Figure 9 shows snapshots of the WT, E13T, E13Q, W32Y and W32A FMN binding protein isoforms.

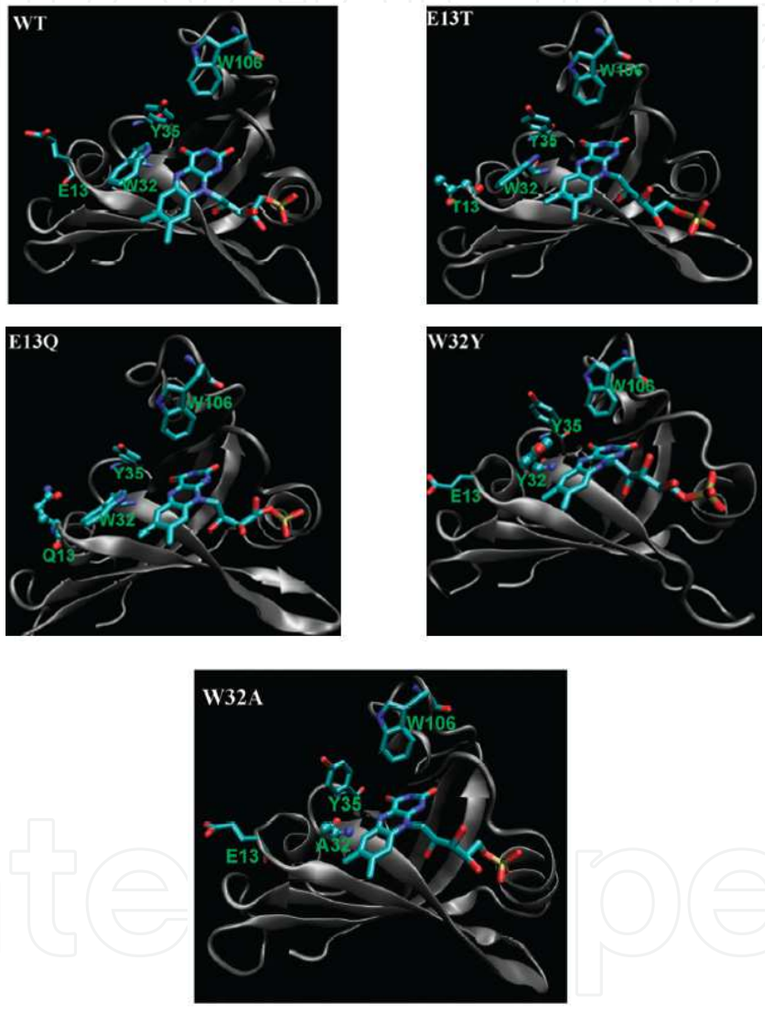

Fig. 9. Protein structures near Iso in the five FMN binding protein isoforms. Trp32, Tyr35 and Trp106 are potential PET donors in the FMN binding protein. Trp32 is replaced by Tyr in W32Y and Ala in W32A. Amino acids at residue position 13 are also shown in the Figures. These structures were obtained by MD simulation.Data were taken from Nunthaboot et al. (2011). (Reproduced by permission of the PCCP Owner Societies).

Mean the donor-acceptor distances over MD time range are summarized in Table 6A, 6B. The WT displays great variations in the Rc distances with long periods, in addition to the instantaneous fluctuations. The mean values of the geometrical factors over the entire MD

time range (2 ns with 0.1 ps time intervals) are listed in Table 6. The Rc distance is shortest in Trp32 among the three different aromatic amino acid residue positions (Trp/tyr32, Tyr 35 and Trp106) with mean distances of Trp32 of 0.70, 0.72 and 0.75 nm in the WT, E13T and E13Q isoforms, respectively. The distance between Iso and Tyr32 in W32Y is shorter than that between Iso and Trp32 in the WT. The inter-planar angle between Iso and Trp32 varies from -52 deg in the WT to -38 deg in the E13Q isoform, while that between Iso and Tyr35 varies from 43 deg in W32A to 93 deg in the WT.

4.1 Amino acid at position 13 of the FMN binding proteins

The WT FMN binding protein contains Glu13, with a negative charge at neutral pH, whilst in the E13T and E13Q substitution isoforms the amino acids at this position are Thr13 and Gln13 with neutral charges. The distances between the PET donors or acceptor and amino acid residue 13 of the five FMN binding protein isomers are listed in Table 7. The distances between Iso and side chain of amino acid 13 do not significantly vary between the five FMN binding protein isoforms (range 1.5 – 1.6 nm), nor does that between Trp32 (0.9 – 1.0 nm), Tyr35 (1.0 – 1.2 nm) and Trp106 (1.7 – 1.97 nm) excepting that of Trp106 in the W32Y isoform that was further away (2.13 nm).

Protein system	Rc (nm)[b]				Re (nm)[b]			
	Trp32	Tyr32	Tyr35	Trp106	Trp32	Tyr32	Tyr35	Trp106
WT	0.703	--	1.016	1.052	0.261	--	0.425	0.314
(RSD[c])	-0.072	--	-0.097	-0.088	-0.086	--	-0.292	-0.29
E13T	0.724	--	0.872	0.913	0.269	--	0.331	0.269
(RSD[c])	-0.048	--	-0.069	-0.038	-0.079	--	-0.181	-0.111
E13Q	0.748	--	0.854	0.939	0.265	--	0.287	0.294
(RSD[c])	-0.044	--	-0.053	-0.043	-0.095	--	-0.123	-0.131
W32Y	--	0.654	0.826	0.907	--	0.276	0.284	0.251
(RSD[c])	--	-0.05	-0.075	-0.036	--	-0.091	-0.167	-0.11
W32A	--	--	0.769	0.895	--	--	0.29	0.277
(RSD[c])	--	--	-0.082	-0.05	--	--	-0.226	-0.139

[a]Mean values of factors between Iso and the nearby indicated aromatic amino acids are listed. The mean values were obtained by taking an average over the entire MD time range.
[b]Center-to-center distance (Rc) and edge-to-edge (Re) distance.
[c]Relative standard deviation (RSD), obtained from SD/mean value.

Table 6A. Geometrical factor of Iso and the indicated nearby aromatic amino acids of the FMN binding protein isomers[a]. Data were taken from Nunthaboot et al. (2011). (Reproduced by permission of the PCCP Owner Societies).

Protein system	Inter-planar angle (deg)			
	Trp32	Tyr32	Tyr35	Trp106
WT	-52.2	--	93.3	67.4
(RSD[c])	(-0.3)	--	(-0.3)	(-0.1)
E13T	-42.5	--	59.3	85.7
(RSD[c])	(-0.2)	--	(-0.2)	(-0.1)
E13Q	-37.8	--	116.4	79.2
(RSD[c])	(-0.2)	--	(-0.1)	(-0.1)
W32Y	--	28.7	76.7	77.5
(RSD[c])	--	(-0.6)	(-0.1)	(-0.1)
W32A	--	--	42.8	70.9
(RSD[c])	--	--	(-0.6)	(-0.1)

Table 6B. Inter-planar angle factor between Iso and the indicated nearby aromatic amino acids of the FMN binding protein isomers[a] Data were taken from Nunthaboot et al. (2011). (Reproduced by permission of the PCCP Owner Societies).

System	Iso	Trp32	Tyr32	Tyr35	Trp106
WT[b]	1.53 ± 0.10	0.98 ± 0.09	--	0.99 ± 0.16	1.72 ± 0.15
E13T[c]	1.49 ± 0.06	0.92 ± 0.07	--	1.22 ± 0.08	1.97 ± 0.09
E13Q[c]	1.58 ± 0.13	0.98 ± 0.12	--	1.12 ± 0.16	1.84 ± 0.17
W32Y[b]	1.64 ± 0.07	--	1.13 ± 0.08	1.46 ± 0.09	2.13 ± 0.09
W32A[b]	1.60 ± 0.11	--	--	1.24 ± 0.15	1.76 ± 0.16

[a]Mean distances (± 1 standard deviation), averaged over the MDS time range, are shown in units of nm.
[b]Distances were obtained taking the average over all distances between atoms in the aromatic ring and the center of the two oxygen atoms in the side chain of Glu13.
[c]Obtained by taking the average over all distances between the atoms in the aromatic ring and the oxygen atom of the Thr13 (E13T) or Gln13 (E13Q) side chain.

Table 7. Geometry of the amino acid residue at position 13 in the five FMN binding protein isoforms[a]. Data were taken from Nunthaboot et al. (2011). (Reproduced by permission of the PCCP Owner Societies).

4.2 The PET rates and related physical quantities in FMN binding proteins

The common parameters among the five FMN binding protein isoforms are listed in Table 3, where ν_0 = 1016 (ps^{-1}) for Trp and 197 (ps^{-1}) for Tyr, β = 21.0 (nm^{-1}) for Trp and 6.25 (nm^{-1}) for Tyr, R_0 = 0.663 (nm) for Trp and 0.499 (nm) for Tyr. G^0_{Iso} = 6.71 (eV) and ε_{DA} = 2.19.

These values are quite different from those of the flavodoxins. The time-evolutions of the PET rates in the five different FMN binding protein isoforms over the MD time course are shown in Figure 10. Fluctuations of the PET rate are always marked in Tyr35, but not so much in Trp32. In the WT isoform the PET rates vary with rather long periods in addition to the instantaneous fluctuations, which is in accord with the time-evolution of Rc distances in the WT. The mean PET rate and physical quantities related to the PET rates are listed in Table 8, where the PET rate is observed to always be fastest from Trp32, and then from Trp106 whilst that from Tyr35 is always slow (see also Figure 10). Among the WT, E13T and

Quantity	Donor	WT	E13T	E13Q	W32Y	W32A
k_{KM}^{jk} [b] (ps^{-1})	Trp32	7.10 ± 3.08	17.22 ± 14.76	10.81 ± 10.43	--	--
	Tyr32	--	--	--	1.6 ± 30 x10^{-7}	
	Tyr35	4 ± 95 x 10^{-14}	6.4 ± 400 x10^{-21}	7 ± 200 x10^{-17}	3.7 ± 200 x10^{-14}	5 ± 130 x 10^{-13}
	Trp106	0.082 ± 0.110	0.003 ± 0.003	0.018 ± 0.011	0.192 ± 0.350	0.176 ± 0.599
λ_S^{jk} [c] (eV)	Trp32	0.202 ± 0.005	0.206 ± 0.004	0.208 ± 0.004	--	--
	Tyr32	--	--	--	0.217 ± 0.005	--
	Tyr35	0.249 ± 0.006	0.240 ± 0.005	0.229 ± 0.004	0.236 ± 0.006	0.231 ± 0.006
	Trp106	0.232 ± 0.005	0.223 ± 0.003	0.225 ± 0.003	0.223 ± 0.002	0.222 ± 0.003
$E_j(k)$ [d] (eV)	Iso	0.071 ± 0.013	-0.023 ± 0.024	0.021 ± 0.028	0.074 ± 0.030	0.079 ± 0.026
	Trp32	0.005 ± 0.017	0.335 ± 0.043	0.269 ± 0.032	--	--
	Tyr32	--	--	--	0.123 ± 0.033	
	Tyr35	0.080 ± 0.025	0.472 ± 0.050	0.391 ± 0.041	0.256 ± 0.052	0.242 ± 0.052
	Trp106	-0.140 ± 0.007	-0.326 ± 0.011	-0.297 ± 0.010	0.141 ± 0.039	0.230 ± 0.054
$ES_j(k)$ [e] (eV)	Trp32	0.076 ± 0.010	0.312 ± 0.027	0.290 ± 0.021	--	--
	Tyr32	--	--	--	0.197 ± 0.020	--
	Tyr35	0.150 ± 0.022	0.449 ± 0.041	0.412 ± 0.035	0.330 ± 0.046	0.321 ± 0.043
	Trp106	-0.069 ± 0.017	-0.349 ± 0.025	-0.276 ± 0.029	0.215 ± 0.034	0.309 ± 0.042
$-e^2/\varepsilon_0^{DA}R_{jk}$ [f] (eV)	Trp32	-0.949 ± 0.055	-0.912 ± 0.045	-0.883 ± 0.045	--	--
	Tyr32	--	--	--	-1.009 ± 0.049	--
	Tyr35	-0.660 ± 0.070	-0.759 ± 0.051	-0.883 ± 0.039	-0.803 ± 0.039	-0.863 ± 0.066

Quantity	Donor	WT	E13T	E13Q	W32Y	W32A
	Trp106	-0.627 ± 0.056	-0.722 ± 0.027	-0.703 ± 0.030	-0.728 ± 0.027	-0.728 ± 0.037
$-\Delta G_T^{0}$ [g] (eV)	Trp32	0.371	0.098	0.090	--	--
	Tyr32	--	--	--	-0.491	--
	Tyr35	-0.792	-0.992	-0.832	-0.829	-0.760
	Trp106	0.194	0.569	0.477	0.011	-0.073

[a] Mean (± SD) values, taken over the MD time range (2 ns with 0.1 ps intervals), are listed. The PET rate is obtained by KM theory.
[b] The PET rate is given by Eq. (4).
[c] Solvent reorganization energy is given by Eq. (2).
[d] ES energy of the Iso anion or the donor cation and other ionic groups, as given by Eq. (7).
[e] Net ES energy, as given by Eq. (8).
[f] ES energy between the Iso anion and a donor cation.
[g] Total standard free energy, as given by Eq. (12).

Table 8. Mean PET rate and its related physical quantities in five FMN binding protein isoforms [a]. Data were taken from Nunthaboot et al. (2011). (Reproduced by permission of the PCCP Owner Societies).

E13Q isoforms, the PET rate from Trp32 was fastest in E13T. The values of λ_S^{jk} do not vary significantly with the donor and protein system (range 0.202 – 0.231 eV). Likewise the ES energies between the Iso anion and the donor cations, $-e^2 / \varepsilon_{DA} R_{jk}$, did not vary much among the donors (range -0.949 eV to -0.627 eV) (Table 8 and Figure 11). In contrast, the net ES energies, $ES_j(k)$, varied from -0.069 eV in Trp106 (WT) to 0.449 eV in Tyr35 (E13T). This remarkable variation in $ES_j(k)$ compared to the other physical quantities is also seen in the flavodoxin isoforms.

4.3 Effect of changing the negative charge of amino acid residue 13 on the PET rate

The PET rate of Trp32 was fastest in all five FMN binding protein isoforms. The ES energies between the Iso anion and ionic groups in the proteins, $E_j(k)$, fell from 0.071 eV in the WT (and similar values in W32Y and W32A) to -0.023 eV and 0.021 eV in E13T and E13Q, respectively (Table 8; Figure 11), suggesting a potential affect of the charge neutralization at residue position 13. In addition, the ES energies between the Trp32 cation and the ionic groups in the proteins increased dramatically from 0.005 eV in the WT, to 0.335 eV and 0.269 eV in the E13T and E13Q isoforms, respectively. In the WT the ES energy between the negative charge of Glu and Trp32 cation should be negative, which contributes to reduce the value of $E_j(k)$. In the neutral charged (at residue 13) E13T and E13Q isoforms the stabilizing energy found in the WT disappears, again supporting the potential importance of the negative charge at residue 13. It is noted that the absolute values of the net ES energies are quite low in the WT, while they are much higher in the other isoforms. Net ES energies of Trp32, from which the PET rate is fastest, are always positive, while those for Trp106 are negative in the WT, E13T and E13Q isoforms.

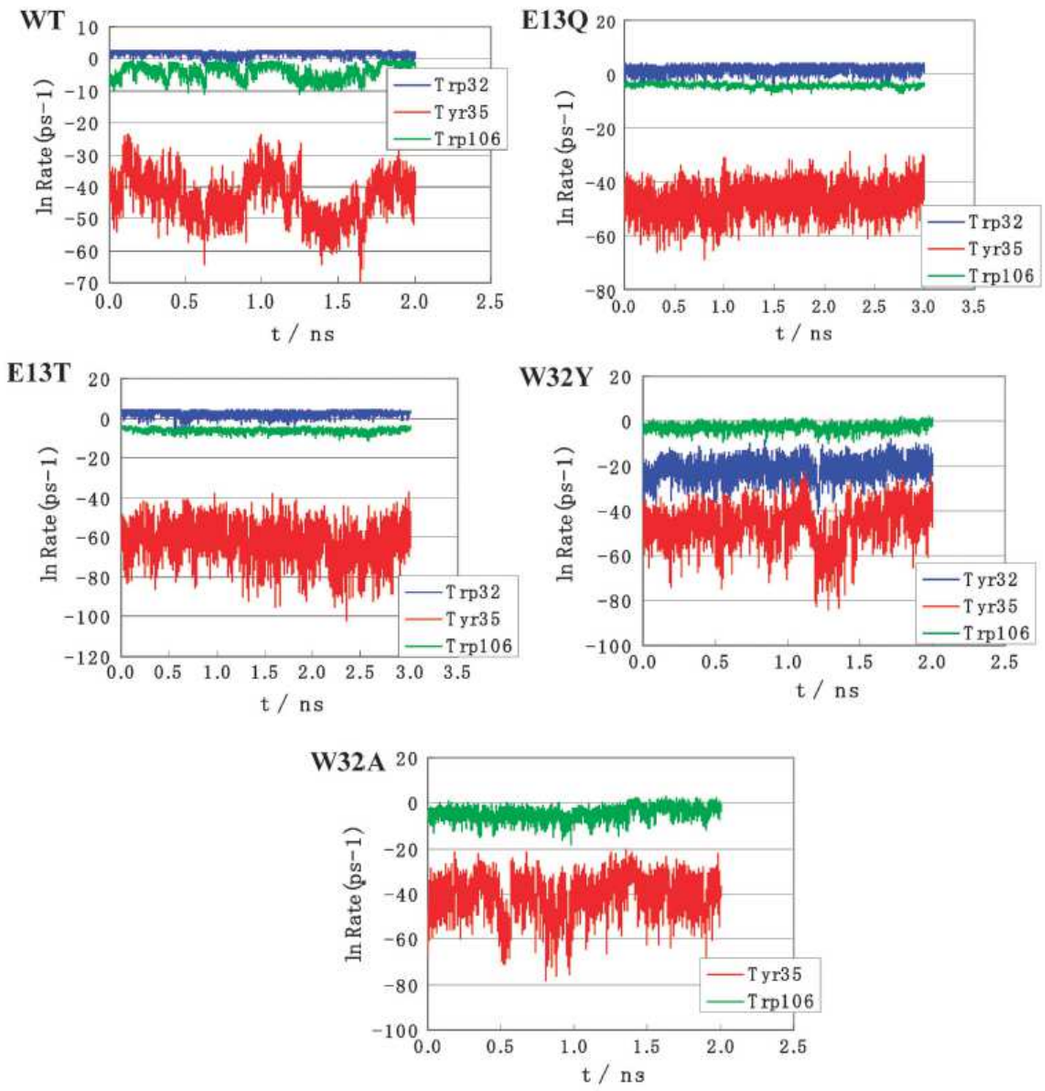

Fig. 10. Time-evolution of the PET rate in the five FMN binding protein isoforms. Data were taken from Nunthaboot et al. (2011). (Reproduced by permission of the PCCP Owner Societies).

5. Energy gap law in flavodoxin and FMN binding protein systems

The total free energy gap of the k^{th} donor in the j^{th} flavoprotein is expressed by Eq. (12);

$$-\Delta G_T^0(jk) \propto -ES_j(k) + e^2 / \varepsilon_{DA} R_{jk} - \Delta G_q^0 \tag{12}$$

When λ_S^{jk} varies with $-\Delta G_T^0(jk)$, the normal energy gap law is modified, as in Eq. (13);

$$\ln k_{KM}^{jk} / \lambda_S^{jk} \propto -\left[\left\{1 + \Delta G_T^0(jk) / \lambda_S^{jk}\right\}^2\right] \tag{13}$$

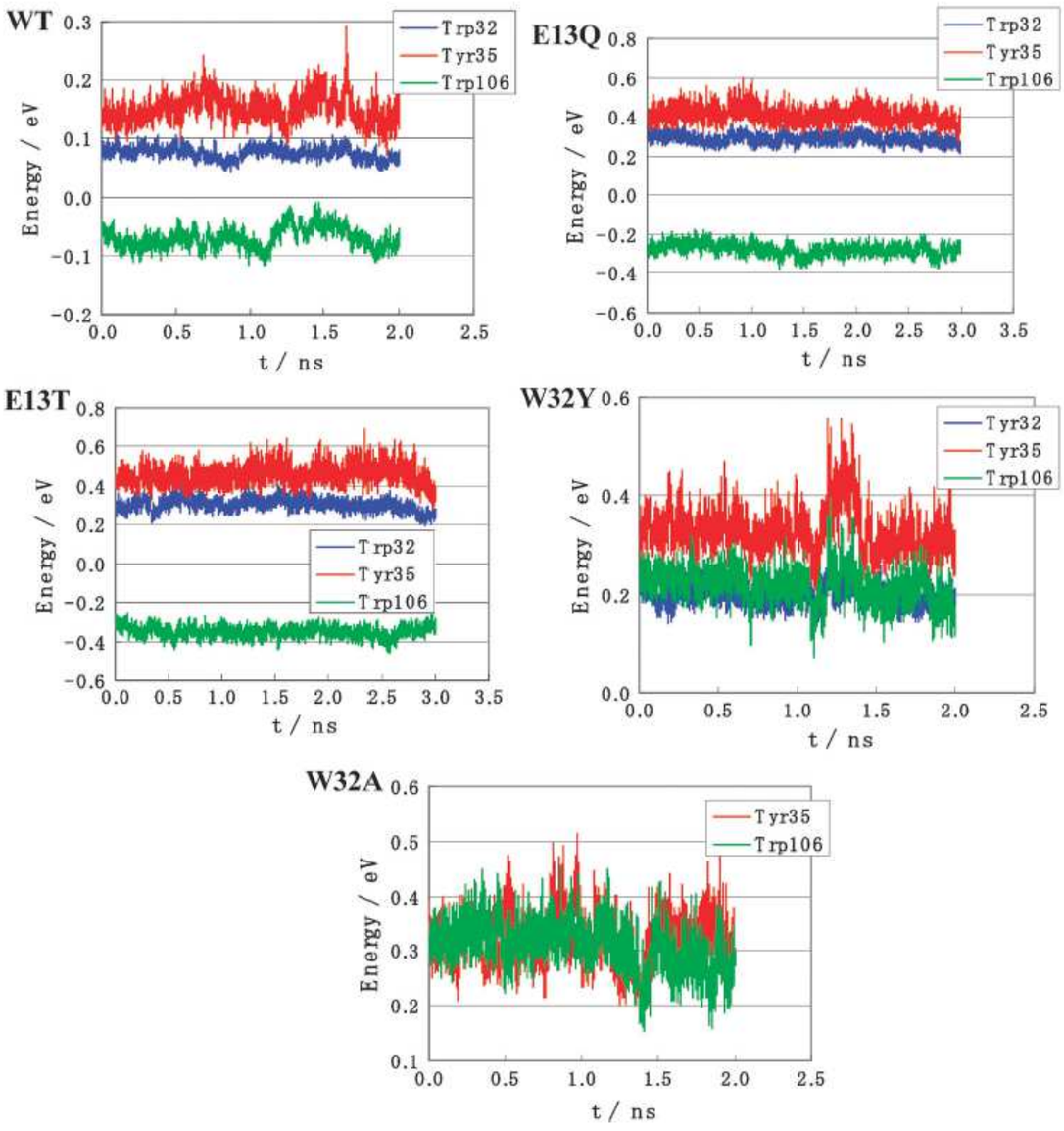

Fig. 11. Net ES energy in the five FMN binding protein isoforms. Data were taken from Nunthaboot et al. (2011). (Reproduced by permission of the PCCP Owner Societies).

Here $ES_j(k)$ is given by Eq. (8), and ΔG_q^0 by Eq. (3). The values of $-\Delta G_T^0(jk)$ are listed in the bottom lines of Table 5 for flavodoxins and Table 8 for FMN binding proteins. Figure 12 shows the modified energy gap law in flavodoxins and FMN binding proteins, as expressed by Eq. (13). The inserts in Figure 12 represent the approximate parabola functions. In the both systems, the PET takes place in the normal region.

6. Concluding remarks on the PET mechanism in flavoproteins

Quantitative analyses of the PET in proteins have been difficult, because all of the current PET theories contain several unknown parameters which cannot be determined experimentally. In the earlier works the PET rate was qualitatively analyzed from the following two aspects.

1. The donor-acceptor distance-dependence of the PET rate (Dutton law).

Hopfield (1974) described biological electron transfer rate in the ground state of a donor in terms of the electron tunneling model. In this model, the rate drops off exponentially with increasing donor-acceptor distance. Hopfield estimated the slope of the logarithm of the rate against the distance to be 14 nm^{-1} for biological electron transfer reactions. Indeed, Moser et al. (1992) have experimentally demonstrated that logarithms of PET rates linearly decrease with the Re distance between PET donors and acceptors in photosynthetic proteins. In accord, the slope of the logarithm of the PET rate against the free energy gap was also around 14 nm^{-1}. Gray & Winkler (1996) have reviewed the experimental works on PET rates in ground state donors from various aspects.

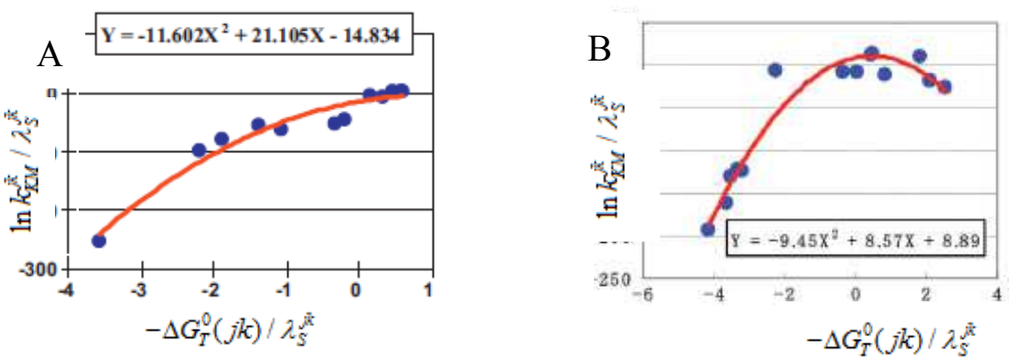

Fig. 12. Modified energy gap law in (A) flavodoxins and (B) FMN binding proteins. Inserts indicate the approximate parabola functions, Y $\ln k_{KM}^{jk} / \lambda_S^{jk}$, and X $-\Delta G_T^0(jk) / \lambda_S^{jk}$. Formally, the value of $\ln k_{KM}^{jk} / \lambda_S^{jk}$ should be maximal when $-\Delta G_T^0(jk) = \lambda_S^{jk}$. Data were taken from Lugsanangarm et al. (2011c) for Figure 12A and Nunthaboot et al. (2011) for Figure 12B. (Reproduced by permission of the PCCP Owner Societies).

2. The free energy gap dependence of PET rate (Energy gap law).

The characteristics of the Marcus theory (1956a, 1956b, 1964) is that the logarithm of the PET rate is a parabolic function of the reorganization energy and the free energy gap (see Eq. (1)), which is common with the other theories (see Eqs. (4) and (5)). As a test for the Marcus theory many researchers have examined the dependence of the logarithmic values of the PET rates on the free energy gap. Rehm & Weller (1969; 1970) first examined the energy gap law with the donor-acceptor systems in organic solvents, but could not find the predicted parabolic dependence. Later Closs et al. (1986) and Mataga et al. (2003) found evidence of the PET processes in the so-called "Inverted region". Interested readers should consult Mataga et al. (2005), who have precisely reviewed the current knowledge of PET in solution.

The energy gap law in proteins was first experimentally demonstrated in the reaction center of the purple bacterium, *Rhodobacter sphaeroides*, by Gunner & Dutton (1989), and in both the plant photosystem I and reaction center of the purple bacterium by Iwaki *et al*. (1996). In these systems, the PET takes place in the normal regions, as in the flavoproteins described above.

We have been trying to quantitatively analyze PET in flavoproteins (Nunthaboot et al., 2008a, 2008b, 2009a, 2009b, 2010, 2011; Lugsanangarm et al., 2011b, 2011c), using the experimental and theoretical approaches of evaluating the ultrafast fluorescence dynamics of Iso in the flavoproteins and using MD simulation based approaches, respectively.The following conclusions have been derived on the mechanisms of PET in the flavoproteins.

1. The donor-acceptor distance-dependent PET rates were analyzed with MH, KM and BJ theories, whereupon the KM theory was found to be the best for describing PET in the flavoproteins.
2. The ultrafast fluorescence decays of flavoproteins are mostly non-exponential. The non-exponential decay of the WT FMN binding protein was first reproduced with MD snapshots and PET theories, taking an average of the single-exponential decay function over the MD time domain (Nunthaboot et al., 2009a). This suggests that the non-exponential behavior in the decays is caused by the fluctuations of the protein structures with short and longer fluctuation periods. Again, KM theory could best reproduce the observed non-exponential decay.
3. The ultrafast experimental decays in several flavoprotein isoforms are satisfactorily reproduced with common PET parameters in the present method (Nunthaboot et al., 2008a, 2010, 2011; Lugsanangarm et al., 2011c).
4. The introduction of ES energy into the PET theories greatly improves the agreement between the observed and (KM theory) calculated decays in the three FMN binding protein isoforms (Nunthaboot et al, 2008a, 2009a).
5. The introduction of the dielectric constant between the donor and acceptor (ε_{DA}) improved the agreement between the observed and (KM theory) calculated decays (Nunthaboot et al., 2011). ε_{DA} is different from the dielectric constant inside the entire protein (ε_0^j), and always much lower than ε_0^j. This is reasonable because normally no amino acid exists between the donor and acceptor.
6. Changes in the single negative charge at residue 13 of the WT FMN binding protein (Glu13) to amino acids with a neutral charge (E13T and E13Q) substantially changed the ultrafast fluorescence decay, which suggests that the ES energy inside the proteins is very important for the PET rate (Chosrowjan et al., 2010; Nunthaboot et al., 2011).

7. Perspective of the quantitative PET analyses

Method of homology modeling has been useful for the determinations of protein structures, which have been experimentally unable (www.proteinstructures.com). The present method for the quantitative analysis of the PET mechanism may be also applicable to photosynthetic systems and flavin photoreceptors, such as AppA (Nunthaboot et al., 2009b; 2010). Most of the flavoproteins function in the electron transport and electron transfer from a substrate to Iso without light. A number of researchers have been working on the mechanisms of the

dark electron transfer in proteins (Grey & Winkler, 1996; Beratan et al., 1991; 2008). These works, however, have mostly focused on the electron coupling term, and not discussed much on the nuclear term. ES energy which is in the nuclear term, should also play an important role on the dark electron transfer rates, and redox potentials of Iso in flavoproteins. Determination of all physical quantities contained in both electronic and nuclear terms of an electron transfer theory could explore a new aspect of the mechanisms of PET and dark electron transfer phenomena in proteins.

8. Acknowledgments

The Royal Golden Jubilee Ph.D. Program (3.C.CU/50/S.1), from Chulalongkorn University and The Thailand Research Fund (TRF) and The Ratchadaphiseksomphot Endowment Fund from Chulalongkorn University are acknowledged for financial support. N. N. (Grant No. MRG5380255) acknowledges the funding for New Research from the Thailand Research Fund. We thank Computational Chemistry Unit Cell, Chulalongkorn University and the National Electronics and Computer Technology Center (NECTEC) for computing facilities. The Thai Government Stimulus Package 2 (TKK2555) under the Project for Establishment of Comprehensive Center for Innovative Food, Health Products and Agriculture and The Higher Education Research Promotion is acknowledged.

9. References

Bendall, D. S. (1996). *Protein Electron Transfer*. BIOS Scientific Publishers Ltd., ISBN 1859960405, Oxford, UK

Beratan, D. N., Betts, J. N. & Ounchic, J. N. (1991). Protein electron transfer rates are predicted to be set by the bridging secondary and tertiary structure, Science, Vol. 252, pp. 1285-1288, ISBN 9780199753833

Beratan, D. N. & Balabin, I. A. (2008). Heme-copper oxidases use tunneling pathways, *Proc. Nat. Acad. Sci. USA,* Vol. 105, pp. 403-404, ISBN 0027-8424

Bixon, M. & Jortner, J. (1991). Non-Arrhenius temperature dependence of electron-transfer rates. *J. Phys. Chem.*, Vol. 95, No. 5, pp. 1941-1944, ISBN 0022-3654

Bixon, M. & Jortner, J. (1993). Charge Separation and Recombination in Isolated Supermolecules. *J. Phys. Chem.*, Vol. 97, No. 50, pp. 13061-13066, ISBN 0022-3654

Bixon, M.; Jortner, J.; Cortes, J.; Heitele, H. & Michelbeyerle, M. E. (1994). Energy-Gap Law for Nonradiative and Radiative Charge-Transfer in Isolated and in Solvated Supermolecules. *J. Phys. Chem.*, Vol. 98, No. 30, pp. 7289-7299, ISBN 0022-3654

Blankenship, R. E. (2002). *Molecular Mechanisms of Photosynthesis*. Wiley-Blackwell, ISBN 0632043210, Oxford, UK

Burkhart, B. M.; Ramakrishnan, B.; Yan, H.; Reedstrom, R. J.; Markley, J. L.; Straus, N. A. & Sundaralingam, M. (1995). Structure of the Trigonal Form of Recombinant Oxidized Flavodoxin from Anabaena-7120 at 1.40 Angstrom Resolution. *Acta Crystallogr D-Biol Cryst*, Vol. 51, No. 3, pp. 318-330, ISBN 0907-4449

Chosrowjan, H.; Taniguchi, S.; Mataga, N.; Tanaka, F.; Todoroki, D. & Kitamura, M. (2007). Comparison between ultrafast fluorescence dynamics of FMN binding protein from

Desulfovibrio vulgaris, strain miyazaki, in solution vs crystal phases. *J. Phys. Chem. B*, Vol. 111, No. 30, pp. 8695-8697, ISBN 1520-6106

Chosrowjan, H.; Taniguchi, S.; Mataga, N.; Tanaka, F.; Todoroki, D.& Kitamura, M. (2008). Ultrafast fluorescence dynamics of FMN-binding protein from *Desulfovibrio vulgaris* (Miyazaki F) and its site-directed mutated proteins. *Chem. Phys. Lett.*, Vol. 462, No. 1-3, pp. 121-124, ISBN 0009-2614

Chosrowjan, H.; Taniguchi, S.; Mataga, N.; Nakanishi, T.; Haruyama, Y.; Sato, S.; Kitamura, M. & Tanaka, F. (2010). Effects of the Disappearance of One Charge on Ultrafast Fluorescence Dynamics of the FMN Binding Protein. *J. Phys. Chem. B*, Vol. 114, No. 18, pp. 6175-6182, ISBN 1520-6106

Closs, G. L.; Calcaterra, L. T.; Green, N. J.; Penfield, K. W. & Miller, J. R. (1986). Distance, stereoelectronic effects, and the Marcus inverted region in intramolecular electron transfer in organic radical anions. *J. Phys. Chem.*, Vol. 90, No. 16, pp. 3673-3683, ISBN 0022-3654

Crosson, S. & Moffat, K. (2001). Structure of a flavin-binding plant photoreceptor domain: insights into light-mediated signal transduction. *Proc. Natl. Acad. Sci. U.S.A.*, Vol. 98, No. 6, pp. 2995-3000, ISBN 0027-8424

Drennan, C. L.; Pattridge, K. A.; Weber, C. H.; Metzger, A. L.; Hoover, D. M. & Ludwig, M. L. (1999). Refined structures of oxidized flavodoxin from Anacystis nidulans. *J. Mol. Biol.*, Vol. 294, No. 3, pp. 711-724, ISBN 0022-2836

Frago, S.; Gomez-Moreno, C. & Medina, M. (2008). *Flavins and Flavoproteins 2008*. Prensas Universitarias de Zaragoza, ISBN 8477330174, Spain

Freigang, J.; Diederichs, K.; Schafer, K. P.; Welte, W. & Paul, R. (2002). Crystal structure of oxidized flavodoxin, an essential protein in *Helicobacter pylori*. *Protein Sci.*, Vol. 11, No. 2, pp. 253-261, ISBN 0961-8368

Fukuyama, K.; Matsubara, H. & Rogers, L. J. (1992). Crystal structure of oxidized flavodoxin from a red alga Chondrus crispus refined at 1.8 A resolution. Description of the flavin mononucleotide binding site. *J. Mol. Biol.*, Vol. 225, No. 3, pp. 775-789, ISBN 0022-2836

Fukuyama, K.; Wakabayashi, S.; Matsubara, H. & Rogers, L. J. (1990). Tertiary structure of oxidized flavodoxin from an eukaryotic red alga Chondrus crispus at 2.35-A resolution. Localization of charged residues and implication for interaction with electron transfer partners. *J. Biol. Chem.*, Vol. 265, No. 26, pp. 15804-15812, ISBN 0021-9258

Giovani, B.; Brydin, M.; Ahmad, M. & Brettel, K. (2003). Light-induced electron transfer in a cryptochrome blue-light photoreceptor. *Nat. Struct. Biol. 10*, pp.489–490, ISBN 0878931686

Gray, H. B. & Winkler, J. R. (1996). Electron transfer in proteins. *Annu. Rev. Biochem.*, Vol. 65, No. 1, pp. 537-561, ISBN 0066-4154

Gunner, M. R. & Dutton, P. L. (1989). Temperature and -.DELTA.G.degree. dependence of the electron transfer from BPh.cntdot.- to QA in reaction center protein from Rhodobacter sphaeroides with different quinones as QA. *J. Am. Chem. Soc.*, Vol. 111, No. 9, pp. 3400-3412, ISBN 0002-7863

Hoover, D. M. & Ludwig, M. L. (1997). A flavodoxin that is required for enzyme activation: The structure of oxidized flavodoxin from Escherichia coli at 1.8 angstrom resolution. *Protein Sci.*, Vol. 6, No. 12, pp. 2525-2537, ISBN 0961-8368

Hopfield, J. J. (1974). Electron Transfer Between Biological Molecules by Thermally Activated Tunneling. *Proc. Natl. Acad. Sci. U.S.A.*, Vol. 71, No. 9, pp. 3640-3644, ISBN 0027-8424

Hush, N. S. (1961). Adiabatic theory of outer sphere electron-transfer reactions in solution. *Trans. Faraday Soc.*, Vol. 57, No. 4, pp. 557-580, ISBN 0014-7672

Iwaki, M.; Kumazaki, S.; Yoshihara, K.; Erabi, T. & Itoh, S. (1996). Delta G(0) dependence of the electron transfer rate in the photosynthetic reaction center of plant photosystem I: Natural optimization of reaction between chlorophyll a (A(0)) and quinone. *J. Phys. Chem.*, Vol. 100, No. 25, pp. 10802-10809, ISBN 0022-3654

Jortner, J. & Bixon, M. (1999). *Electron Transfer—from Isolated Molecules to Biomolecules, in Advances in Chemical Physics: Electron Transfer - from Isolated Molecules to Biomolecules. Part 1*. John Wiley & Sons, Inc., ISBN 9780471252924, Hoboken, NJ, U.S.A.

Kakitani, T. & Mataga, N. (1985). New energy gap laws for the charge separation process in the fluorescence quenching reaction and the charge recombination process of ion pairs produced in polar solvents. *J. Phys. Chem.*, Vol. 89, No. 1, pp. 8-10, ISBN 0022-3654

Kakitani, T.; Yoshimori, A. & Mataga, N. (1991). Theoretical Analysis of Energy-Gap Laws of Electron-Transfer Reactions, In: *Electron Transfer in Inorganic, Organic, and Biological Systems,* pp. 45-69, American Chemical Society, ISBN 0-8412-1846-3

Kakitani, T.; Yoshimori, A. & Mataga, N. (1992). Effects of the donor-acceptor distance distribution on the energy gap laws of charge separation and charge recombination reactions in polar solutions. *J. Phys. Chem.*, Vol. 96, No. 13, pp. 5385-5392, ISBN 0022-3654

Karen, A.; Ikeda, N.; Mataga, N. & Tanaka, F. (1983). Picosecond laser photolysis studies of fluorescence quenching mechanisms of flavin: a direct observation of indole-flavin singlet charge transfer state formation in solutions and flavoenzymes. *Photochem. Photobiol.*, Vol. 37, No. 5, pp. 495-502, ISBN 0031-8655

Karen, A.; Sawada, M. T.; Tanaka, F. & Mataga, N. (1987). Dynamics of excited flavoproteins-picosecond laser photolysis studies. *Photochem. Photobiol.*, Vol. 45, No. 1, pp. 49-54, ISBN 1751-1097

Kita, A.; Okajima, K.; Morimoto, Y.; Ikeuchi, M. & Miki, K. (2005). Structure of a Cyanobacterial BLUF Protein, Tll0078, Containing a Novel FAD-binding Blue Light Sensor Domain. *J. Mol. Biol.*, Vol. 349, No. 1, pp. 1-9, ISBN 0022-2836

Kitamura, M.; Kojima, S.; Ogasawara, K.;Nakaya, T.; Sagara, T.; Niki, K.; Miura, K.;Akutsu, H. & Kumagai, I. (1994). Novel FMN-binding protein from *Desulfovibrio vulgaris* (Miyazaki F). Cloning and expression of its gene in Escherichia coli. *J. Biol. Chem.*, Vol. 269, No. 8, pp. 5566-5573, ISBN 0021-9258

Kitamura, M.; Sagara, T.; Taniguchi, M.; Ashida, M.; Ezoe, K.; Kohno, K.; Kojima, S.; Ozawa, K.; Akutsu, H.; Kumagai, I. & Nakaya, T. (1998). Cloning and expression of the

gene encoding flavodoxin from *Desulfovibrio vulgaris* (Miyazaki F). *J. Biochem.*, Vol. 123, No. 5, pp. 891-898, ISBN 1756-2651

Laan, W.; van der Horst, M. A.; van Stokkun, I. H. M. & Hellingwerf, K. (2003). Initial Characterization of the Primary Photochemistry of AppA, a Blue-light–using Flavin Adenine Dinucleotide–domain Containing Transcriptional Antirepressor Protein from *Rhodobacter sphaeroides*: A Key Role for Reversible Intramolecular Proton Transfer from the Flavin Adenine Dinucleotide Chromophore to a Conserved Tyrosine? *J. Photochem. Photobiol.*, *78*, 290–297, ISBN 1010-6030.

Liepinsh, E.; Kitamura, M.; Murakami, T.; Nakaya, T. & Otting, G. (1997). Pathway of chymotrypsin evolution suggested by the structure of the FMN-binding protein from *Desulfovibrio vulgaris* (Miyazaki F). *Nat. Struct. Mol. Biol.*, Vol. 4, No. 12, pp. 975-979, ISBN 1072-8368

Ludwig, M. L.; Pattridge, K. A.; Metzger, A. L.; Dixon, M. M.; Eren, M.; Feng, Y. C. & Swenson, R. P. (1997). Control of oxidation-reduction potentials in flavodoxin from Clostridium beijerinckii: The role of conformation changes. *Biochemistry*, Vol. 36, No. 6, pp. 1259-1280, ISBN 0006-2960

Lugsanangarm, K.; Pianwanit, S.; Kokpol, S. & Tanaka, F. (2011a). Homology modelling and molecular dynamics simulations of wild type and mutated flavodoxins from *Desulfovibrio vulgaris* (Miyazaki F): insight into FMN–apoprotein interactions. Mol. Simulat., Vol. 37, No. 14, pp. 1164-1178, ISBN 0892-7022

Lugsanangarm, K.; Pianwanit, S.; Kokpol, S.; Tanaka, F.; Chosrowjan, H.; Taniguchi, S. & Mataga, N. (2011b). Analysis of photoinduced electron transfer in flavodoxin. *J. Photochem. Photobiol. A: Chem.*, Vol. 217, No. 2-3, pp. 333-340, ISBN 1010-6030

Lugsanangarm, K.; Pianwanit, S.; Kokpol, S.; Tanaka, F.; Chosrowjan, H.; Taniguchi, S. & Mataga, N. (2011c). Photoinduced electron transfer in wild type and mutated flavodoxin from *Desulfovibrio vulgaris*, strain Miyazaki F.: Energy gap law. *J. Photochem. Photobiol. A: Chem.*, Vol. 219, No. 1, pp. 32-41, ISBN 1010-6030

Marcus, R. A. (1956a). On the Theory of Oxidation-Reduction Reactions Involving Electron Transfer. I *J. Chem. Phys.*, Vol. 24, No. 5, pp. 966–978, ISBN 0021-9606

Marcus, R. A. (1956b). Electrostatic Free Energy and Other Properties of States Having Nonequilibrium Polarization. I. *J. Chem. Phys.*, Vol. 24, No. 5, pp. 979-989, ISBN 0021-9606

Marcus, R. A. (1964). Chemical and Electrochemical Electron-Transfer Theory. *Annu. Rev. Phys. Chem.*, Vol. 15, No. 1, pp. 155-196, ISBN 0066-426X

Marcus, R. A. & Sutin, N. (1985). Electron transfers in chemistry and biology. *Biochim. Biophys. Acta.*, Vol. 811, No. 3, pp. 265-322, ISBN 0304-4173

Masuda, S. & Bauer, C. E. (2002). AppA is a blue light photoreceptor that antirepresses photosynthesis gene expression in Rhodobacter sphaeroides. *Cell*, Vol. 110, No. 5, pp. 613-623, ISBN 0092-8674

Masuda, S., Hasegawa, K., Ishii, A. & Ono, T. (2004). Light-Induced Structural Changes in a Putative Blue-Light Receptor with a Novel FAD Binding Fold Sensor of Blue-Light Using FAD (BLUF); Slr1694 of Synechocystis sp. PCC6803. *Biochemistry*, Vol. 43, No. 18, pp. 5304-5313, ISBN 0006-2960

Mataga, N.; Chosrowjan, H.; Shibata, Y. & Tanaka, F. (1998). Ultrafast fluorescence quenching dynamics of flavin chromophores in protein nanospace. *J. Phys. Chem. B*, Vol. 102, No. 37, pp. 7081-7084, ISBN 1089-5647

Mataga, N.; Chosrowjan, H.; Shibata, Y.; Tanaka, F.; Nishina, Y. & Shiga, K. (2000). Dynamics and mechanisms of ultrafast fluorescence quenching reactions of flavin chromophores in protein nanospace. *J. Phys. Chem. B*, Vol. 104, No. 45, pp. 10667-10677, ISBN 1089-5647

Mataga, N.; Chosrowjan, H.; Taniguchi, S.; Tanaka, F.; Kido, N. & Kitamura, M. (2002). Femtosecond fluorescence dynamics of flavoproteins: Comparative studies on flavodoxin, its site-directed mutants, and riboflavin binding protein regarding ultrafast electron transfer in protein nanospaces. *J. Phys. Chem. B*, Vol. 106, No. 35, pp. 8917-8920, ISBN 1520-6106

Mataga, N.; Taniguchi, S.; Chosrowjan, H.; Osuka, A. & Yoshida, N. (2003). Ultrafast charge separation and radiationless relaxation processes from higher excited electronic states of directly linked porphyrin-acceptor dyads. *Photochem. Photobiol. Sci.*, Vol. 2, No. 5, pp. 493-500, ISBN 1474-905X

Mataga, N.; Taniguchi, S.; Chosrowjan, H.; Osuka, A. & Kurotori, K. (2005). Observations of the whole bell-shaped energy gap law in the intra-molecular charge separation (CS) from S-2 state of directly linked Zn-porphyrin-imide dyads: Examinations of wider range of energy gap (-ΔGcs) for the CS rates in normal regions. *Chem. Phys. Lett.*, Vol. 403, No. 1-3, pp. 163-168, ISBN 0009-2614

Mataga, N.; Chosrowjan, H. & Taniguchi, S. (2005). Ultrafast charge transfer in excited electronic states and investigations into fundamental problems of exciplex chemistry: Our early studies and recent developments. *J. Photochem. Photobiol. C Photochem. Rev.*, Vol. 6, No. 1, pp. 37-79, ISBN 1389-5567

McCormick, D. B. (1977). Interactions of flavins with amino acid residues: assessments from spectral and photochemical studies. *Photochem. Photobiol.*, Vol. 26, No. 2, pp. 169-182, ISBN 1751-1097

Moser, C. C.; Keske, J. M.; Warncke, K.;Farid, R. S. & Dutton, P. L. (1992). Nature of biological electron transfer. *Nature*, Vol. 355, No. 6363, pp. 796-802, ISBN 0028-0836

Nunthaboot, N.; Tanaka, F.; Kokpol, S.; Chosrowjan, H.; Taniguchi, S. & Mataga, N. (2008a). Simultaneous analysis of ultrafast fluorescence decays of FMN binding protein and its mutated proteins by molecular dynamic simulation and electron transfer theory. *J. Phys. Chem. B*, Vol. 112, No. 41, pp. 13121-13127, ISBN 1520-6106

Nunthaboot, N.; Tanaka, F.; Kokpol, S.; Chosrowjan, H.; Taniguchi, S. & Mataga, N. (2008b). Quantum mechanical study of photoinduced charge transfer in FMN binding protein. *J. Phys. Chem. B*, Vol. 112, No. 49, pp. 15837-15843, ISBN 1520-6106

Nunthaboot, N.; Tanaka, F.; Kokpol, S.; Chosrowjan, H.; Taniguchi, S. & Mataga, N. (2009a). Simulation of ultrafast non-exponential fluorescence decay induced by electron transfer in FMN binding protein. *J. Photochem. Photobiol. A: Chem.*, Vol. 201, No. 2-3, pp. 191-196, ISBN 1010-6030

Nunthaboot, N.; Tanaka, F. & Kokpol, S. (2009b). Analysis of photoinduced electron transfer in AppA. *J. Photochem. Photobiol. A: Chem.*, Vol. 207, No. 2-3, pp. 274-281, ISBN 1010-6030

Nunthaboot, N.; Tanaka, F. & Kokpol, S. (2010). Simultaneous analysis of photoinduced electron transfer in wild type and mutated AppAs. *J. Photochem. Photobiol. A: Chem.*, Vol. 209, No. 1, pp. 79-87, ISBN 1010-6030

Nunthaboot, N.; Pianwanit, S.; Kokpol, S. & Tanaka, F. (2011). Simultaneous analyses of photoinduced electron transfer in the wild type and four single substitution isomers of the FMN binding protein from *Desulfovibrio vulgaris*, Miyazaki F. *Phys. Chem. Chem. Phys.*, Vol. 13, No. 13, pp. 6085-6097, ISBN 1463-9076

Rehm, D.; Weller, A. & Bunsen., B. (1969). Kinetics and mechanism of electron transfer in fluorescence quenching in acetonitrile. *Ber. Bunsenges, Phys. Chem.*, Vol. 73, No. 1, pp. 834 – 839

Rehm, D. & Weller, A. (1970). Kinetics of fluorescence quenching by electron and hydrogen-atom transfer. *Isr. J. Chem.*, Vol. 8, No. 1, pp. 259 - 271

Sancho, J. (2006). Flavodoxins: sequence, folding, binding, function and beyond. *Cell. Mol. Life Sci.*, Vol. 63, No. 7-8, pp. 855-864, 1420-682X

Silva, E. & Edwards, A. M. (2006). *Flavins: Photochemistry and Photobiology*. RSC Publishing, ISBN 0-85404-331-4, Cambridge, London

Sumi, H. & Marcus, R. A. (1986). Dynamical effects in electron transfer reactions *J. Chem. Phys.*, Vol. 84, No. 9, pp. 4894-4914, ISBN 00219606

Suto, K.; Kawagoe, K.; Shibata, N.; Morimoto, Y.; Higuchi, Y.; Kitamura, M.; Nakaya, T. & Yasuoka, N. (2000). How do the X-ray structure and the NMR structure of FMN-binding protein differ? *Acta Crystallogr. D*, Vol. 56, No. 3, pp. 368-371, ISBN 0907-4449

Tanaka, F.; Chosrowjan, H.; Taniguchi, S.; Mataga, N.; Sato, K.; Nishina, Y. & Shiga, K. (2007). Donor-acceptor distance-dependence of photoinduced electron-transfer rate in flavoproteins. *J. Phys. Chem. B*, Vol. 111, No. 20, pp. 5694-5699, ISBN 1520-6106

Tanaka, F.; Rujkorakarn, R.; Chosrowjan, H.; Taniguchi, S. & Mataga, N. (2008). Analyses of donor-acceptor distance-dependent rates of photo-induced electron transfer in flavoproteins with three kinds of electron transfer theories. *Chem. Phys.*, Vol. 348, No. 1-3, pp. 237-241, ISBN 0301-0104

van der Berg, P. A. & Visser, A. J. W. G. (2001). *New Trends in Fluorescence Spectroscopy. Applications to Chemical and Life Sciences*. First ed.; Springer, ISBN 3540677798, Berlin

Vogler, A.; Scandola, F.; Rehorek, D. & Kunkely, H. (2011). *Photoinduced Electron Transfer (Topics in Current Chemistry)*. Springer, ISBN 3540525688, Berlin

Vorsa, V.; Kono, T.; Willey, K. F. & Winograd, N. (1999). Femtosecond Photoionization of Ion Beam Desorbed Aliphatic and Aromatic Amino Acids: Fragmentation via α-Cleavage Reactions. *J. Phys. Chem. B*, Vol. 103, No. 37, pp. 7889-7895, ISBN 1520-6106

Watenpaugh, K. D.; Sieker, L. C. & Jensen, L. H. (1973). The binding of riboflavin-5'-phosphate in a flavoprotein: flavodoxin at 2.0-Angstrom resolution. *Proc. Natl. Acad. Sci. U.S.A.*, Vol. 70, No. 12, pp. 3857-3860, ISBN 0027-8424

Weber, G. (1950). Fluorescence of riboflavin and flavin-adenine dinucleotide. *Biochem. J.*, Vol. 47, No. 1, pp. 114–121

Zhong, D. P. & Zewail, A. H. (2001). Femtosecond dynamics of flavoproteins: Charge separation and recombination in riboflavine (vitamin B-2)-binding protein and in glucose oxidase enzyme. *Proc. Natl. Acad. Sci. U.S.A.*, Vol. 98, No. 21, pp. 11867-11872, ISBN 0027-8424

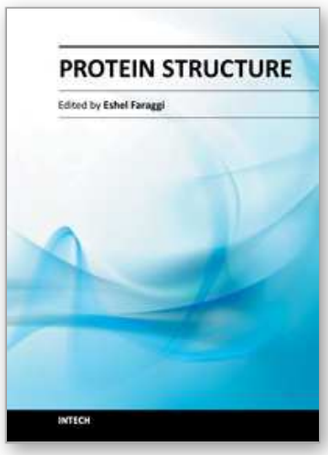

Protein Structure
Edited by Dr. Eshel Faraggi

ISBN 978-953-51-0555-8
Hard cover, 396 pages
Publisher InTech
Published online 20, April, 2012
Published in print edition April, 2012

Since the dawn of recorded history, and probably even before, men and women have been grasping at the mechanisms by which they themselves exist. Only relatively recently, did this grasp yield anything of substance, and only within the last several decades did the proteins play a pivotal role in this existence. In this expose on the topic of protein structure some of the current issues in this scientific field are discussed. The aim is that a non-expert can gain some appreciation for the intricacies involved, and in the current state of affairs. The expert meanwhile, we hope, can gain a deeper understanding of the topic.

How to reference
In order to correctly reference this scholarly work, feel free to copy and paste the following:

Kiattisak Lugsanangarm, Nadtanet Nunthaboot, Somsak Pianwanit, Sirirat Kokpol and Fumio Tanaka (2012). Theoretical Analyses of Photoinduced Electron Transfer from Aromatic Amino Acids to the Excited Flavins in Some Flavoproteins, Protein Structure, Dr. Eshel Faraggi (Ed.), ISBN: 978-953-51-0555-8, InTech, Available from: http://www.intechopen.com/books/protein-structure/theoretical-analyses-of-photoinduced-electron-transfer-from-aromatic-amino-acids-to-the-excited-flav

INTECH
open science | open minds

InTech Europe
University Campus STeP Ri
Slavka Krautzeka 83/A
51000 Rijeka, Croatia
Phone: +385 (51) 770 447
Fax: +385 (51) 686 166
www.intechopen.com

InTech China
Unit 405, Office Block, Hotel Equatorial Shanghai
No.65, Yan An Road (West), Shanghai, 200040, China
中国上海市延安西路65号上海国际贵都大饭店办公楼405单元
Phone: +86-21-62489820
Fax: +86-21-62489821

IntechOpen